



CHALMERS
UNIVERSITY OF TECHNOLOGY

Assessment of upper extremity movements in persons with stroke using a inertial navigation system

A validation study using motion capture

Master's thesis in Biomedical engineering

Joakim Sundberg

Assessment of upper extremity movements in persons with stroke using a inertial navigation system

A validation study using motion capture

Joakim Sundberg

Department of of signals and systems

Chalmers University of Technology

Abstract

Stroke ranks the top number five cause of lost disability-adjusted-life-years in poor and middle-income countries, and impaired motor function on one side of the body is reported to be present in 80% of the cases. Correct assessment of the motor function in survivors have been shown to play a important part in successful rehabilitation. Previous works have reported that the kinematic variables total movement time, trunk displacement and movement smoothness have high correlation with clinical scales, such as Action Research Arm Test when derived from the every-day task of drinking from a glass of water. Kinematic movement analysis is classically performed using a sophisticated motion capture system, which may be unsuitable for small practises or poor countries. This thesis presents and evaluates the design of a system created to measure the motor impairment in the upper limbs of stroke survivors using only a cheap IMU and a standard computer.

A motion capture system using a verified method to derive the two variables movement smoothness and total movement time was used in conjunction with an IMU mounted on the subjects wrist. The study used a population of 16 subjects, out of which 3 subjects were affected by motor impairment due to stroke, for a total of 186 trials. A readily developed navigation algorithm using a unscented Kalman filter fitted with a smoother was used to estimate the trajectory and speed of the IMU. A novel algorithm was developed to derive the total movement time and movement smoothness from the IMU estimate. Using linear regression models, the IMU systems estimate of smoothness predicted the motion capture systems corresponding variable with a RMSE of 2.15 and R^2 of 0.83. The estimates of the movement smoothness showed a notable disparity in the two systems, especially when derived from stroke survivors. The IMU system would need considerable rise in overall performance to create a next to perfect match. The movement time showed a high level of correlation, with a RMSE of 0.45. Developing a method to also estimate the trunk-displacement variable and use it together with the two existing estimates would be the next step in improving the method.

Keywords: Stroke rehabilitation, navigation, UKF, kinematic analysis, INS

Acknowledgements

This work was performed at Acreo Swedish ICT with the aid of the Institute of Neuroscience and Physiology, at the Sahlgrenska Academy, University of Gothenburg.

I'd like extend thanks my two supervisors and my examiner: Jan Wipenmyr at Acreo, Margit Murphy at the Institute of Neuroscience and Physiology, Sahlgrenska Academy, and Tomas McKelvey at the Dep. of Signals and Systems, Chalmers. Particularly for insight, optimism and, lets not forget, a liberal dose of patience.

Special thanks to Peter Björkholm at Acreo for aid and perspective.

Joakim Sundberg, Gothenburg, May 2016

Contents

List of Figures	x
List of Tables	xi
1 Introduction	1
1.1 Background	2
1.2 Problem statement	3
1.3 Scope	3
2 Theory	5
2.1 Assessment of upper extremity function and activity after stroke . . .	6
2.2 State estimation	6
2.2.1 Kalman filters	7
2.2.2 The unscented kalman filter	8
2.2.3 Smoothing	9
2.2.4 Dead reckoning, inertial navigation & available information . .	9
2.3 Sensors	11
2.3.1 Accelerometer	12
2.3.2 Gyroscope	12
2.4 Attitude representation	12
3 Methodology	15
3.1 Overview: procedure, data acquisition and verification	16
3.2 Experimental procedure	16
3.3 Kinematic measures	18
3.4 Inertial Measurement System: Velocity & trajectory estimation . . .	19
3.5 Parameter extraction	19
3.5.1 MCS: Movement units & TMT	20
3.5.2 IMUS: Movement units	20
3.5.3 IMUS: Total time	22
3.6 Hardware	22
3.7 Statistical methods	23
3.7.1 Linear regression	23
3.8 Population and recruitment	24
3.8.1 Inclusion and exclusion criteria for individuals with stroke . .	24
3.8.2 Inclusion and exclusion criteria for healthy individuals	25

4	Results	27
4.1	Estimation quality and robustness	28
4.2	Linear regression analysis	34
5	Discussion	37
6	Conclusion	41
	Bibliography	43
A	Appendix 1	I
A.1	Moments of MU-sets	II
A.2	Polynomial and linear regression-models	III
A.3	Scatterplots	VIII
A.4	Linear regression graphs	X

Abbreviations

ARAT	Action Research Action Test
FMA-UE	Fugl-Meyer Assessment for Upper Extremity
FNMU	Filtered Number of measurement Units (NMUs derived from filtered data)
Hx	Healthy subject nr. x
INS	Inertial navigation system
KF	Kalman Filter
MCS	Motion Capture System (referring to the hard- and software used to derive the NMU and TMT variables)
IMUS	Inertial Measurement Unit System (referring to the hard- and software used to derive the NMU and TMT variables)
NMU	Number of measurement Units
RMSE	Root Mean Square Error
Sx	Subject nr.x affected by stroke
TMT	Total Movement Time
UKF	Unscented Kalman Filter

List of Figures

3.1	The magnitude and phase response of the Butterworth filter.	20
3.2	Estimated Total Movement Time by the IMUS from accelerometer data	21
4.1	A pair of estimates from a healthy subject (H110), made by the MCS and IMUS, where the estimate of the IMUS contains small errors with respect to other estimates.	29
4.2	A pair of estimates from a healthy subject (H110), made by the MCS and IMUS, where the estimate of the IMUS deviates and show noticeable errors. An example of a worse estimate with respect to other IMUS estimates.	31
4.3	A pair of estimates from a subject with stroke (S201), made by the MCS and IMUS, where the estimate of the IMUS contains small errors with respect to other estimates.	32
4.4	A pair of estimates from a subject with stroke, made by the MCS and IMUS (S201), where the estimate of the IMUS deviates and show noticeable errors. An example of a worse estimate with respect to other IMUS estimates.	33
4.5	Barplots featuring the standard-deviation of the MU features for all data.	34
A.1	FNMU scatter/bar-plots of the affected and healthy samples respectively.	VIII
A.2	NMU scatter/bar-plots of the affected and healthy samples respectively.	IX
A.3	Scatterplots of the three different features.	X
A.4	Regression models predicting MCS:NMU using IMUS:FNMU.	XI
A.5	Regression models predicting MCS:NMU using IMUS:NMU.	XII

List of Tables

3.1	The different variable names and sample-sets used. Can be combined in 15 different sets. Inertial Measurement Unit System (IMUS, refers to both hardware and algorithms), Motion Capture System (refers to both hardware and algorithms), Number of Movement Units (NMU), Filtered Number of Movement Units (FNMU, NMUs calculated from low-pass filtered data), Total Movement Time (TMT).	17
3.2	The phases of the drinking task	18
3.3	Specs of the sensors in the IMU	23
3.4	The healthy participants of the study-population	24
3.5	The stroke participants of the study-population	25
4.1	Most common differences between the IMUS and MCS speed estimates.	30
4.2	Mean RMSE and R^2 for polynomial and linear regression models created using 10-fold cross-validation on all a affected (14) samples and a equal number of random healthy samples (14). Total 28 samples.	35
4.3	Mean and population standard deviation for the kinematic variables sorted by level of motor-impairment.	35
A.1	Moments of the sets for the MU-variables, on the form mean \pm std. . .	II
A.2	Notation of set-divisions used to detail the moments of the MU-distributions	III
A.3	Notation of set-divisions used to train and test regression models . . .	III
A.4	Performance of linear regression for NMU with NMU as predictor . .	IV
A.5	Performance of linear regression for NMU with FNMU as predictor .	V
A.6	Performance of linear regression with for TMT	VI
A.7	Performance of polynomial regression models using FNMU as training data to predict NMU	VII

1

Introduction

1.1 Background

Roughly 15 million people suffer from stroke worldwide annually, out of which 5 million are permanently disabled [1]. The disease is more common in poor and middle-income countries, as opposed to high-income countries. The former has been calculated to carry 87% of the burden of stroke, measured in disability-adjusted life years (DALYs), where it also ranks the top number five cause of lost DALYs [2]. Impaired motor function and movement control on one side of the body is a common side-effect of stroke, reported to be present in 80% of the cases. Disability in the upper limbs have been reported to occur in up to 70% of the cases, out of which 40% suffer from impaired upper extremity function 3-6 months after the event [3]. A persons quality of life can be severely affected due to such neural damage, which commonly result in inability to perform everyday tasks and participate in society [4].

Rehabilitation is the multi-disciplinary process of attempting to achieve and retaining optimal function in interaction with the environment despite experienced disability. It relies on both physical and psychological processes to heal or compensate for loss of function [5, 3]. Correct assessment and evaluation play a part in this, since factors such as goals and motivation affect the clinical outcomes of the rehabilitation. The approach of choice is to use observational rating scales. That is, to rely on tests with weighted scoring to determine parameters describing control, sensor/motor function and pain in the upper limbs. The area of assessment and application of the tests vary, leading to the existence of a number of tests, such as ABILHAND, Fugl-Meyer Assessment and the Action Research Arm Test (ARAT). Typical equipment range from forms to dynamometers, stopwatches and objects of different weights or shapes [6, 7, 3].

Kinematic movement analysis refers to the practice of analysing the speed and movement patterns of a subject. The term implies the use of pictures, cinematography or in modern days, computer-based analysis of either. In rehabilitation, kinematic movement analysis can be used in tandem with classical approaches to quantify motor function or detect discrepancies in the subjects health. The field is historically strongly related to gait analysis in which it has seen a success and is well documented and explored. In upper extremity analysis it is less so due to the more complex and less predictable nature of the uses of the upper limbs. It's as of yet mostly used for research purposes, though a number of approaches and variables have been explored. For the purposes of measuring the effects of stroke, a number of variables have been show to correlate. Velocity, movement time, smoothness, movement errors and trunk displacement amongst others have been reported in the literature [8, 3].

Traditional optoelectrical hardware for kinematic movement analysis can be unsuitable for at-home measurements or installation at small practices due to lack of user friendliness and pricing. The trend of diminishing prices for computational power and high quality sensors have however opened up for the possibility to use cheaper equipment, heralding an era of more accessible data-collection. The use of

inertial sensors (accelerometers and gyroscopes) have seen use in physiotherapy and been applied in various smart textile applications [9, 11, 10]. The data can either be used in raw form, or used to estimate the corresponding velocities via inertial navigation. The latter opening up for applying the methodology of kinematic movement analysis.

1.2 Problem statement

The aim is to design an algorithm which derives kinematic parameters from a reach-to-drink-task as described in [3], using only a 3-DOF gyroscope and accelerometer. Furthermore, to evaluate the correlation between the new set of parameters and the corresponding parameters from the already evaluated motion capture system defined in the latter. This is to be done by evaluating the precision prediction models constructed using the two sets of parameters. The two parameters to be estimated are the Number of Movement Units (NMU) and Totalt Movement Time (TMT), as defined in [3]. The overall purpose is to determine whether a INS presents a feasible substitute for a optoelectrical system using the approach and algorithms presented in [3].

1.3 Scope

- To choose a INS approach substituting that of the optoelectrical system.
- To create a set of algorithms deriving two parameters from the substitute trajectory/velocity-vector estimating the MU and TMT measures.
- To evaluate the mimicked parameters precision and usefulness as predictors against the true parameters.

2

Theory

2.1 Assessment of upper extremity function and activity after stroke

Motor impairment after stroke is the restriction of effective and coordinated movement on one side of the body. A number of deficits contribute to the state: muscle weakness, spasticity, muscle stiffness, loss of sensory functions and reduced muscle length among them. The majority of the improvements after stroke occur in the first few months, and greatly affected patients commonly have a slower rate of rehabilitation [3]. While patients motor functions change over time, greater differences can be found between different people. This creates a situation where different scales become necessary, since, much like a sensor, the scales sensitivity and range are interconnected.

The ARAT measures upper extremity function and dexterity on a 0-57 point scale (57 indicating normal motor performance). It uses a 4-point ordinal scale on 19 different items, divided into the categories of grasp, grip, pinch and gross movement. The scale is considered valid for motor assessment in both chronic and acute care. In the act of drinking from a glass of water (see section 3.2) two groups of variables have shown significant correlation with ARAT, compensatory movement and smoothness/movement time. Compensatory movement includes measures of joint angles and trunk displacement, with trunk displacement showing the highest correlation of the two. Smoothness (measured in NMU, see section 3.2) and movement time have been shown to be roughly interchangeable. 67% of the variance of ARAT has been shown to be explained by the trunk displacement and the NMU of the subject when using a multiple regression model. [3].

2.2 State estimation

States are variables which partially or wholly describe the dynamics of a system. That is, describing the relations between the input(s), output(s) and time. State estimation refers to the practice of through modelling of systems, sensors and disturbances attempt to calculate states of interest from input and output measurements. The scope of the modelling (the states needed to describe the system sufficiently), modelling of stochastic processes and attenuation of noise are all examples of challenges in the field. Noise is ever-present in sensors and signals, while models rarely describe the dynamics of systems perfectly, making the goal of the field to describe and minimize errors rather than finding exact answers.

A common tool for mathematical modelling of systems is the (discrete) state-space representation, as seen in equation 2.1 and 2.2. Where x represent the state-vector, which contains the state variables. The index k represent the time instance, q the state-noise, y the output and r the measurement noise. The symbols f and h are the system and measurement models of the system. A useful abstraction of the state estimation problem is to divide it into the following problems: prediction, filtering

and smoothing. The three problems are defined by at which temporal instances the estimates are calculated. Prediction uses data to predict states several time-instances away, filtering uses the current data to estimate the current state and smoothing estimate the states in previous time instances. [12]

$$x_k = f_{k-1}(x_{k-1}, q_{k-1}) \quad (2.1)$$

$$y_k = h_k(x_k, r_k) \quad (2.2)$$

2.2.1 Kalman filters

The Kalman filter was invented around 1960, and has seen major use in a number of fields ever since. Navigation and orientation estimation among them. Nowadays a great number of variations exist, making the original Kalman filter redundant for all but simpler applications or education purposes. A vast amount of literature and publications exist on the subject, for more detailed information the reader is urged to look at sources such as [16], [15], [14] and [17]. The Kalman filter is a optimal linear state observer, i.e. an algorithm using a linear mathematical model of a real system to estimate states at every time instance k , using only previous measurements up until time instance k . Optimal refers to that the filter creates an optimal estimate of the states in a MSE sense if the measurement and system noise is Gaussian. The filter use models on the form of equation 2.3 and 2.4.

$$x_k = A_{k-1}x_{k-1} + B_{k-1}u_{k-1} + q_{k-1} \quad (2.3)$$

$$y_k = H_kx_k + r_k \quad (2.4)$$

That is, modelling the states x as a linear combination of previous states propagated through model A , previous input u through model B with additive noise q . The measurements y are similarly estimated using the measurement model H , the estimated states of the current timestep x and additive noise r .

The algorithm works in two steps, prediction and update. In the prediction step, the states are propagated in accordance with the system model (eq. 2.5) and the uncertainties are increased (2.6).

$$\hat{x}_{k|k-1} = A_{k-1}\hat{x}_{k-1|k-1} \quad (2.5)$$

$$P_{k|k-1} = A_{k-1}P_{k-1|k-1}A_{k-1}^T + Q_{k-1} \quad (2.6)$$

In the update step, the difference (innovation) v between the states created using measurements and the estimated states is weighted by the Kalman gain K and added to the estimate. This creates a state estimate relying on both modelled behaviour and sensor measurements (eq. 2.7).

$$\hat{x}_{k|k} = \hat{x}_{k|k-1} + K_k v_k \quad (2.7)$$

The last step of the algorithm consists of adjusting the covariance matrix P in accordance with the Kalman gain and innovation covariance S .

$$P_{k|k} = P_{k|k-1} - K_k S_k K_k^T \quad (2.8)$$

- A : Transition matrix.
- \hat{x} : Estimated state vector.
- P : Covariance matrix.
- q & r : Process and measurement noise with covariance matrices Q and R .
- H : Measurement model.
- K : Kalman gain, optimal gain for the correction/innovation
- v : innovation, the difference between predicted states and states calculated using the measurements.
- S : innovation covariance.

2.2.2 The unscented kalman filter

The Kalman filter is the optimal solution for linear models only. A number of solutions have been presented aiming to generalise the filter to nonlinear problems. A popular approach is to estimate the moments of the distributions of the states and measurements, creating so-called Gaussian filters. A Gaussian filter creates a number of sigma-points (weighted samples) around the estimated mean of the states and thereby attempt to describe the system in terms of uncertainties and means rather than classical models. Prediction is thus the new estimated mean, created with weighted sigma-points (W and χ) as seen in equations 2.9 and 2.10.

$$\hat{x}_{k|k-1} = \sum_{i=0}^{2n} f(\chi_{k-1}^i) W_i \quad (2.9)$$

$$P_{k|k-1} = \sum_{i=0}^{2n} f(\chi_{k-1}^i - \hat{x}_{k|k-1})(\chi_{k-1}^i - \hat{x}_{k|k-1})^T W_i + Q_{k-1} \quad (2.10)$$

The update-step consists of estimating the input using sigma-points and the measurement-model. Cross-covariance and innovation is then calculated (equations: 2.11, 2.12 & 2.13).

$$\hat{y}_{k|k-1} = \sum_{i=0}^{2n} h(\chi_{k-1}^i) W_i \quad (2.11)$$

$$P_{xy} = \sum_{i=0}^{2n} f(\chi_{k-1}^i - \hat{x}_{k|k-1})(h(\chi_{k-1}^i) - \hat{y}_{k|k-1})^T W_i \quad (2.12)$$

$$S_k = R_k + \sum_{i=0}^{2n} (h(\chi_{k-1}^i) - \hat{y}_{k|k-1})(\bullet)^T W_i \quad (2.13)$$

The Gaussian Kalman filters are generally named after the method used to approximate the distribution, in this case using the unscented transform. This is not an optimal solution, but the method has proven to be computationally efficient and to be highly competitive in terms of precision.

2.2.3 Smoothing

The smoothing problem refers to the (optimal) estimation of states when measurements and input data exists for future time-instances relative the current estimate. Three varieties of the problem exist,

- Fixed-interval smoothing, the entire input-data set exists.
- Fixed lag smoothing, the next k instances of input-data exists.
- Fixed point smoothing, the states at a fixed time are re-estimated for each new point of collected data.

One of the first solutions formulated to solve the (linear) fixed-interval smoothing problem was the Rauch-Tung-Striebel smoother (for historical purposes, released 1965 [18]). That is, estimating the posteriori distribution given the entire data set (eq. 2.14). The smoother performs backward recursion by using all estimated and predicted means and covariances ($\hat{x}_{k+1|k}$, $\hat{x}_{k|k}$, $P_{k|k}$ & $P_{k+1|k}$) from an ordinary Kalman filter (eq. 2.15, 2.16 & 2.17). [22].

$$p(x_k | y_{1:K}) = N(x_k; \hat{x}_{k|K}, P_{k|K}) \quad (2.14)$$

$$G_k = P_{k|k} A_k^T P_{k+1|k}^{-1} \quad (2.15)$$

$$\hat{x}_{k|K} = \hat{x}_{k|k} + (\hat{x}_{k+1|K} - \hat{x}_{k+1|k}) \quad (2.16)$$

$$P_{k|K} = P_{k|k} - (P_{k+1|k} - P_{k+1|K}) G_k^T \quad (2.17)$$

2.2.4 Dead reckoning, inertial navigation & available information

Navigation is the field of estimating positions from available data. Dead reckoning is a sub-field of navigation in which navigation is performed without the aid of absolute references. Inertial navigation refers to using the classical laws of motion to calculate position by integration of measured speed or acceleration. In practice, a Inertial Navigation System (INS) uses two sensors, a 3-DOF accelerometer (measuring acceleration, including the earths gravitational vector, in its own frame of

reference) and a gyroscope (measuring rotational speed in its own frame of reference). See chapter 2.3 for more information on sensors. In its basic components, a INS operates in the following steps

- Estimate its rotation by integration of the gyroscope measurements. eq. 2.20
- Change the accelerometer measurements frame of reference using the attitude estimate. eq. 2.19
- Remove the earths gravitational vector from the accelerometer measurements. Note that a errors in the attitude estimate will result in imperfect removal of the gravity vector in this step.
- Integrate its accelerometer measurements twice. eq. 2.18

$$\overleftarrow{r}_g^{\ddot{}} = \overleftarrow{f}_g + \overleftarrow{g}_g \quad (2.18)$$

$$\overleftarrow{f}_g + \overleftarrow{g}_s = C(\overleftarrow{f}_s + \overleftarrow{g}_s) \quad (2.19)$$

$$\dot{C} = C\Omega_s \quad (2.20)$$

- \overleftarrow{r} : The position vector.
- \overleftarrow{f} : Measured acceleration.
- \overleftarrow{g} : Gravitational vector
- g & s: global and system frame of reference.
- C: Directional cosine matrix.
- Ω : Skew symmetric matrix containing the gyroscope measurements.

An INS fitted with a 3-DOF accelerometer and gyroscope need to estimate or assume its starting orientation. If the sensor bias is small and the system is assumed to be at rest, the accelerometer can be used to determine orientation in two dimensions using the earths gravitational vector. This is useful since an INS is dependent on accurate initial conditions and measurements - no error can be removed without an absolute reference. Sensor calibration and errors estimation are thus of high importance. Complex systems usually fuse inertial sensors and sensor systems with absolute references to create precise systems with the capability of removing accumulated errors with set intervals. [19].

2.3 Sensors

The cost of sensor precision and computational power has decreased to the point where it's possible to perform navigation using a (relatively) cheap set of devices. A popular approach due to its low cost and electricity consumption is the use of IMUs, defined as a device capable of measuring specific forces and angular rates using inertial sensors. Most efficient sensor-systems require the estimation of sensor errors, since most sensors are affected by errors drifting over time. Complex error models and more computational power can compensate for some sensor errors. Sensor calibration (estimation and compensation of errors) is performed by using a known input and comparing it with the measured input. Precise calibration commonly need to use specific calibration routines, however, on-line calibration is sometimes also possible. Common error models for accelerometers and gyroscopes are presented in eq. 2.22 & 2.21. All errors can be compensated for, but the zero-mean random noise n . [19].

$$\tilde{\omega}_x = (1 + S_x)\omega_x + M_y\omega_y + M_z\omega_z + B_f + B_{gx}a_x + B_{gz}a_z + B_{axz}a_ya_z + n_x \quad (2.21)$$

- $\tilde{\omega}$: Measured turn-rate.
- ω : Actual turn rate around the x-, y- and z-axes.
- S_x : Scale-factor, proportional to input.
- M : Cross-coupling error-factors, errors due to misalignment of sensor-axes.
- B_f : Bias insensitive to the gravitational vector.
- $B_{gx/z}$: Bias due to the gravitational vectors effect on the different axes.
- B_{axz} : Anisoelastic bias, created by faulty suspension structure in spinning-mass gyroscopes.
- n : Zero-mean random bias.

$$\tilde{a}_x = (1 + S_x)a_x + M_ya_y + M_zz + B_f + n_x \quad (2.22)$$

- \tilde{a} : Measured acceleration.
- a : Actual acceleration along the x-, y- and z-axes.
- S_x : Scale-factor, proportional to input.
- M : Cross-coupling error-factors, errors due to misalignment of sensor-axes.
- B_f : Measurement bias.
- n : Zero-mean random bias.

2.3.1 Accelerometer

An accelerometer is by definition a device measuring acceleration along one or more axes. The sensor can be classified as either a mechanical or solid-state device. Mechanical accelerometers principle of operation is based on Newton's second law of motion, and is realised by measuring the translational motion of a proof of mass suspended by springs. Solid-state devices relates stress/compression of materials to the applied forces, commonly by measuring changes of frequency of vibrations generated in the materials. [19].

2.3.2 Gyroscope

A gyroscope is a sensor either measuring the angular displacement of a structure or its angular rate of turn. A conventional rate-gyroscope uses a spinning mass to capitalise on the principle of conservation of angular momentum. Other common methods for measuring angular rates and positions include optical (using the Sagnac effect) and vibratory. [19].

2.4 Attitude representation

A central concept of inertial navigation is that of reference frames. The rotation of a body is described as the difference between an original, fixed, reference system and a rotated body coordinate system. The IMU measurements are all in the body reference frame, centred in the IMU and rotating with it. Most widely used reference frames are orthogonal, right-handed systems. Common representations include the DCM and euler angels. In navigation and state-estimation however, neither are practical to use. The DCM use 9 parameters to describe a 3-dimensional rotation, which is computationally inefficient. The Euler angle representation can create non-unique representations of rotation, which is suboptimal.

The quaternion representation is a compact and efficient representation of attitude which has seen extensive use within navigation, computer graphics and other fields. The quaternion can be described as a representation of a rotation in three dimensions about a single vector v , with a magnitude of v and x-, y- & z-components v_x , v_y & v_z (eq. 2.23). It's commonly expressed as a four-parameter complex number on the form seen in eq. 2.24. The product of two quaternions is called the Hamilton product, and obey the distributive law and the normal laws of multiplication of complex numbers. The quaternion conjugate, magnitude and normalization are described in eq. 2.26, 2.27 and 2.28. The derivative as a function of rates, a very interesting quantity of the quaternion in navigation and state estimation, is described in eq. 2.29. A 3-dimensional vector can be transformed between two frames of reference, represented by a quaternion, as described in eq. 2.25, if the vector is represented as a quaternion without scalar (letting the vectors x-, y- and z-components represent the quaternion a-, b- and c-components). [19].

$$\overleftarrow{q} = \begin{bmatrix} \cos(v/2) \\ (v_x/v) \sin(v/2) \\ (v_y/v) \sin(v/2) \\ (v_z/v) \sin(v/2) \end{bmatrix} \quad (2.23)$$

$$q = [a, ib, jc, kd] \quad (2.24)$$

$$\overleftarrow{r}_g = qr_s q^* \quad (2.25)$$

$$q^* = [a, -ib, -jc, -kd] \quad (2.26)$$

$$N(q) = \sqrt{qq^*} \quad (2.27)$$

$$q_{normalized} = \frac{q}{N(q)} \quad (2.28)$$

$$\dot{q} = 0.5q[0, \omega^T]^T \quad (2.29)$$

3

Methodology

3.1 Overview: procedure, data acquisition and verification

The IMUS (Inertial Measurement System) performance was evaluated by attempting to re-create clinically valid kinematic measures of a system/method of known performance - the MCS (Motion Capture System). Both abbreviations refer to complete procedures, including hardware and algorithms used to derive kinematic variables. This was achieved by collecting data using the two system simultaneously, the IMUS and the MCS, deriving two sets of kinematic measures and evaluating the sets for correlation. The measures and procedure to be evaluated against is based on previous works, in which a procedure has been developed with capability to extract measures with high correlation with impaired motor function in the upper limbs due to stroke [3]. The measures are a quantified measure of smoothness (calculated as number of movement units in the velocity profile, NMU) and total movement-time [3].

The measurement units used was a shimmer3 IMU with a 3-dof accelerometer and gyroscope (IMUS), and a 3-dimensional motion capture system (MCS) installed at Sahlgrenska University Hospital. The relation between the two systems was evaluated in by determining the predictive power of the IMUS against the MCS using linear regression models. For that purpose, a similar test-procedure as described [3] was used. It involved the task of drinking water while acquiring corresponding sets of data from the MCS and the IMUS simultaneously. The kinematic measures were extracted from the MCS as described in [3]. A method was developed for estimating corresponding kinematic measures from the IMUS data. The predictive power of the IMUS was evaluated by designing sets of uni-variate linear regression models between different sets of data from the systems and evaluating the resulting precision and curve-fit. The steps of the validation process and their corresponding methodology-subchapters are as follows:

1. Data collection. **Sections:** 3.6, 3.8 & 3.2.
2. Reconstruct velocity vector and trajectory. **Sections:** 3.6
3. Extraction of kinematic measures. **Sections:** 3.5, 3.3 & 3.6
4. Construction of regression models and evaluation of curve-fit. **Sections:** 3.7.1, 3.7 & 3.8
5. Evaluation of results and conclusion.

3.2 Experimental procedure

The procedure aimed to collect data in paired sets from the two systems, i.e each drinking task recorded by the MCS is paired with the IMUS recording from the same trial. The paired sets were later used to predict the MCS measures from the

Variables	Samples
IMUS:NMU	Healthy
IMUS:FNMU	Stroke
IMUS:TMT	All
MCS:NMU	
MCS:TMT	

Table 3.1: The different variable names and sample-sets used. Can be combined in 15 different sets. Inertial Measurement Unit System (IMUS, refers to both hardware and algorithms), Motion Capture System (refers to both hardware and algorithms), Number of Movement Units (NMU), Filtered Number of Movement Units (FNMU, NMUs calculated from low-pass filtered data), Total Movement Time (TMT).

IMUS data using linear regression. The data used for this purpose is structured by variable name and from which samples it's created, as can be seen in table 3.1. Less commonly used notations are found in the appendix and are only relevant for other tables in the appendix (see Table A.2 and Table A.3).

The measurement procedure consisted of a reach-to-drink task where the subject reached for a glass, took a sip of water and returned the glass to its original position before returning the arm to its starting position. The movement was self-paced. The subject was seated with approximately 90 degrees flexion of the knee joints, sitting in a height-adjustable chair behind a table. The back was in contact with the backrest, the arm to be examined resting with the hand on the table palm facing down and with approximately 90 degrees flexion of the elbow. The 9 spherical MCS markers were placed on the following locations of the subject's body and glass using double-sided tape:

- Third metacarpophalangeal joint (hand of interest).
- Styloid process of ulna (wrist of interest)
- Lateral epicondyle (elbow of interest)
- Middle parts of acromion (both shoulders)
- Upper part of the sternum (thorax)
- Notch between eyebrows (face)
- Upper and lower edge of the glass on the opposite side of the subject

The IMU was strapped on the dorsal side of the lower arm, between the ulna and radius, a few centimetres proximal of the wrist-marker. The glass had a diameter of 7 cm and height of 9.5 cm. It was placed 30 centimetres from the table edge of the subject along the midline of the body, and filled with 75-100 ml of water. Each subject repeated the movement when instructed a total of 10

Phases	Start criterion
Reaching and grasping	The speed of the hand marker exceeds 2% of its top speed between start and the estimated middle of the drinking phase
Forward transport	Speed of the object-marker exceeds $15 \cdot 10^{-2}$ m/s
Drinking	The time at which the object marker is closer to the face marker than the mean distance of the middle 50 samples of the time at which the elbow is within 5 % of maximal flexion + $15 \cdot 10^{-2}$ m
Back transport	The time at which the object marker is further from the face marker than the mean distance of the middle 50 samples of the time at which the elbow is within 5 % of maximal flexion + $5 \cdot 10^{-2}$ m
Return	The point at which the object's speed is less than $1 \cdot 10^{-2}$, looking from the point at which the distance between the wrist and object marker exceeds $1 \cdot 10^{-2}$ m
End	Speed of the hand marker is less than 2% of its top speed between the estimated middle of the drinking phase and end for the last time

Table 3.2: The phases of the drinking task

to 20 times for each arm, with the starting arm being chosen randomly. The start and end position wasn't defined with precision, nor the alignment of the hand or wrist. The procedure was, with respect to marker-positions, the drinking task and sitting position of the subject, identical to that defined in reference [3]. The experimental procedure was changed for subject S2 (Subject nr. 2 affected by stroke), who was unable to properly grasp the glass due to poor motor function (FMA-UE score less than 32). The subject grasped the glass using only two digits, the index and the thumb, as opposed to other subjects whom grasped and drunk using their entire hand. The glass was not filled with water in the case of S2.

3.3 Kinematic measures

The kinematic measures used for verifying the IMUS performance against that of the MCS are a quantified estimate of movement smoothness (Number of Movement Units, NMU, defined in section 3.5.1, derived from the wrist) and Total Movement Time (TMT, beginning and end of the phases defined in Table 3.2) in a reach-to-drink task. The measures have been reported to have significant correlation with ARAT (see section 2.1) and discriminate between discrete levels (moderate, mild and none) of impaired motor function in the upper limbs due to stroke, defined by FMA-UE scores of 32-57 (moderate) and 58-66 (mild) [21][20][3][13]. Together, these measures can create one out of two prominent features for estimating upper limb motor deficiency, the other one being trunk displacement [3].

3.4 Inertial Measurement System: Velocity & trajectory estimation

The IMUS is a dead reckoning system which estimates the trajectory and velocity from the gyroscope and accelerometer data, from which an estimated set of kinematic measures is derived. The system uses a smoother to improve its accuracy, based on an Unscented Kalman Filter (UKF) due to the non-linear nature of the navigation equations [14][19]. Numerical stability and computational efficiency is improved using a square-root implementation [17]. Furthermore, the system decreases some of the errors arising from its lack of absolute reference by assuming the start and stop velocity is zero (Zero Velocity Updating, ZUPT). The state vector is as follows

$$x_k = \begin{bmatrix} q \\ p \\ \dot{p} \\ bias_{acc} \\ bias_{gyro} \\ s_{acc} \end{bmatrix}$$

assuming additive Gaussian noise, using the Q-matrix (process noise, see Chapter: 2.2.2):

$$Q = diag \begin{bmatrix} ones(4, 1) \cdot (V_{\Omega} \cdot T)^2 \\ ones(3, 1) \cdot (\frac{V_A}{2} \cdot T^2)^2 \\ ones(3, 1) \cdot (V_A \cdot T)^2 \\ ones(3, 1) \cdot (V_a^b \cdot T)^2 \\ ones(3, 1) \cdot (V_g^b \cdot T)^2 \\ (T \cdot V_s)^2 \end{bmatrix}$$

The commands are written using Matlab syntax and the variables are defined as Quaternion (q), Position (p), Acceleration scale factor (s), sampling interval (T) & Variance (V). The measurement model assumes no control input, and thus estimate both accelerometer and gyroscope data (see chapter: 2.2.1). Further assumptions are that the IMU's body coordinate system is aligned with the world coordinate system at start and that the system is at rest before navigation starts.

3.5 Parameter extraction

The IMUS attempts to emulate the approaches used by the MCS. It uses the same definition as the MCS to define movement units, but lack the necessary information to calculate the phases of the movement as defined in [3]. The MCS calculates the TMT using an algorithm applicable by the IMUS, since it only uses the speed of the wrist. However, the IMUS estimates the TMT using a novel algorithm less prone to outliers.

Velocity and acceleration vectors of the MCS are estimated with a first order forward finite difference approximation from the measured positions. The estimates are low-pass filtered using a second order Butterworth-filter to remove noise and errors introduced by the velocity and acceleration estimation. Magnitude and phase response of the filter is given in Figure 3.1.

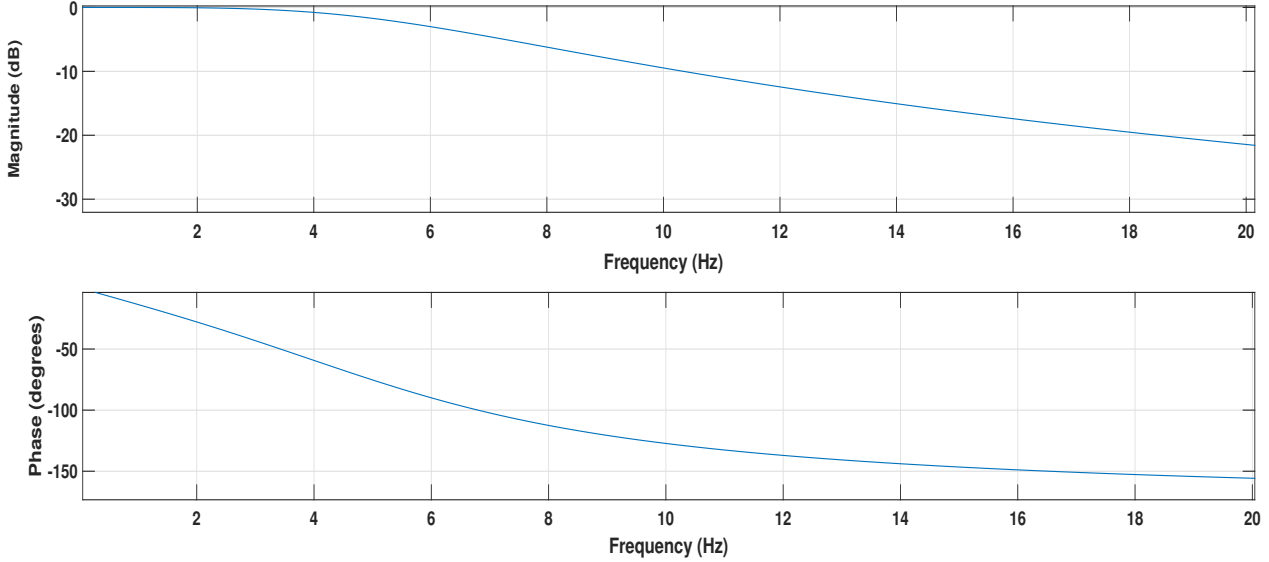


Figure 3.1: The magnitude and phase response of the Butterworth filter.

3.5.1 MCS: Movement units & TMT

The NMU measure was calculated from the magnitude of the velocity vector (speed) of the wrist marker with the help of the positions of the elbow, shoulder, face and object-markers. NMU is defined as the sum of points in the reaching, forward transport, back transport and returning phase (defined in table 3.2) full-filling the following criteria: magnitude greater than adjacent points, magnitude difference greater than $2 \cdot 10^{-3}$ m/s with respect to adjacent MUs and occurring more than $15 \cdot 10^{-2}$ s apart. TMT is defined as the time between the first and last phase (table: 3.2).

3.5.2 IMUS: Movement units

The IMUS derives two different estimates of the NMU, Filtered Number of Movement Units (FNMU) and ordinary NMU. The approach used by the IMUS to estimate the NMU & FNMU measures differs only in the phase-estimation stage from that of the MCS. An algorithm based only on the movement of the wrist was developed and used:

1. Estimate the middle of the motion by finding the highest estimated position along the z-axis (i.e, the point where the wrist is highest above the table. This

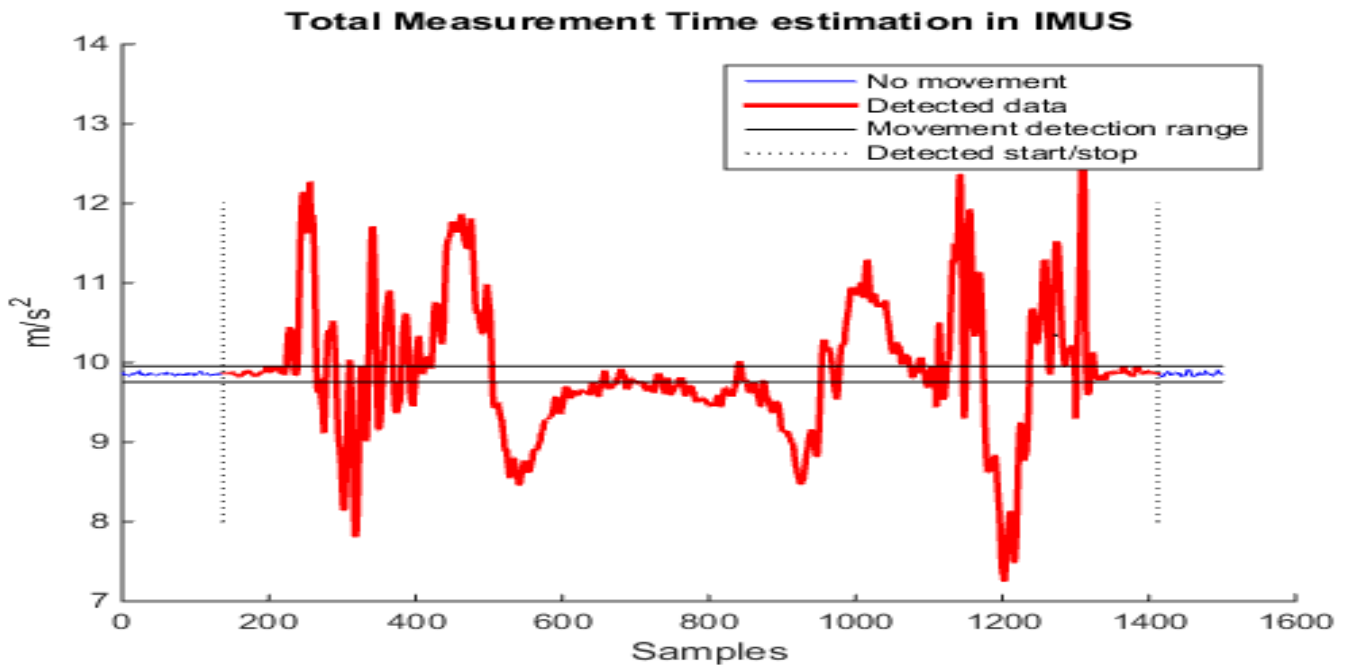


Figure 3.2: Estimated Total Movement Time by the IMUS from accelerometer data

point corresponds to the point where the MCS calculates maximum flexion of the elbow.

2. From point (1) to end, calculate at which point the maximum value of the x-axis is achieved (i.e a point close to where the glass is placed in the return phase). Calculate maximum speed of the wrist along this trajectory.
3. From point (2) to end, calculate the last point at which the object moves with more speed than 5 % of the speed calculated in (2). This corresponds to the time between the Return and End phases.
4. From point (2) to beginning, calculate the last point (from point 2) at which the objects speed is greater than 5 % of the top speed within the interval. This estimates the beginning of the reach phase.
5. From point (1), find the first point within 250 samples (1.22 seconds) in each direction at which point the object moves with speed greater than the speed in (1) + 0.2 m/s. This estimates the drinking phase.

The algorithm relies on a few key assumptions, for example that the wrist reaches its highest point along the z-axis of the world coordinate system during the drinking-phase. Relative measures are used in order to prevent errors due to sub-optimal navigation. In the case of the FNMU, the navigated data is filtered using the MCS's Butterworth filter. This is the only difference between the two parameters. This is an arbitrary solution based on the MCS's algorithm, addressing the problem of outlier sensitivity. The definition of the movement unit states that any single point

with sufficient temporal difference from other movement units and magnitude from adjacent samples is a movement unit. Low energy noise is thus indistinguishable from true movement units, possibly warranting a low-pass filtering of the data to ensure its relevance.

3.5.3 IMUS: Total time

The algorithm used by the MCS to estimate TMT is prone to outliers, since it defines (table: 3.2) the start and stop times as the first and last time the magnitude of the velocity vector exceeds a percentage of the magnitude in another point. A movement recorded before the actual trial start would thus lead to a premature starting point. While the MCS record data only after being activated through Qualisys Track Manager, the IMUS records several trials in a row. The IMUS thus also records movements between the trials and needs to be robust against outliers. The IMUS system uses a decision algorithm capitalising on the fact that the TMT's standard deviation and mean is known from [3].

1. Calculate the magnitude of the accelerometer vector for every point.
2. Estimate g + accelerometer bias by taking the mean of the first 100 samples of the magnitude vector with a sample variance less than $4.6 * 10^{-4}$ (a threshold determined by trial and error using the shimmer3 IMU).
3. Find every point containing movement data, defined as every point with a magnitude deviating from the estimated mean with more than 0.1.
4. Sum the data created in (3), consisting of only zeroes and ones, over a 40 samples wide window running over the entire set. For each summation larger than 3, set all samples within the window to 1. Set all windows not full-filling the criteria to zero.
5. Sum the data created in (4), consisting of only zeroes and ones, over a 1000 samples wide window running over the entire set. For each summation larger or equal to 950, set all samples within the window to 1. Set all windows not full-filling the criteria to zero. Each sample containing a 1 is now considered data, while all other samples (containing 0) are outliers.

3.6 Hardware

The MCS data-acquisition hardware is a optoelectric system produced by Qualisys (ProReflex MCU240). It consists of five cameras with sampling rate of 240 Hz and has sub-millimeter spatial precision. The position data collected is stored and handled by Qualisys Track Manager. The software for estimating velocity, acceleration and kinematic measures is written in Matlab (Mathworks inc).

	Accelerometer	Gyroscope
Range	+/- 4g	+/- 250 dps
Sensitivity	1000 LSB/g at +/- 2g	131 dps/g at +/- 250 dps
Numerical Resolution	16-bit	16-bit
RMS noise	$27.5 \cdot 10^{-3} m/s^2$	0.0481 dps

Table 3.3: Specs of the sensors in the IMU

The Inertial Measurement System (IMUS) consisted of a Shimmer3 (produced by Shimmer) IMU using its 3-dof accelerometer and gyroscope with precision given in table 3.3. The data acquired by the IMUS is imported to Matlab where the trajectory and velocity vectors are estimated using a square-root Unscented Kalman Filter.

3.7 Statistical methods

3.7.1 Linear regression

The methodology is designed to evaluate how much the extracted parameters of the IMUS and MCS correlates. To this purpose, linear regression models (uni-variate linear models and polynomial models of the second degree) are designed using data from the IMUS and the corresponding MCS data. The polynomial models are only used as a predictor for the NMU with the FNMU as training data. A choice based on the FNMU feature's superiority as a predictor. The models fit and precision are evaluated, which indicates if the data-sets correlates in the way described by the models. Model fit and precision is evaluated using the R^2 statistic and RMSE. In order to explore trends and relationships between sub-sets of the data, the models are designed by and applied to different sets of data, with primary focus on the difference between the sets "healthy", "affected" and "all". More intricate comparisons are also made and can be found in the appendix. The sub-sets choices are based on which data is expected to differ from other data - data from a subject with stroke is expected to differ from that of a healthy individual. Due to adverse effects on the results in combination with the modified procedure (more details can be found in the result and discussion chapters), S2 is not included in any set unless explicitly specified. In order to avoid over-fitting, 10-fold cross-validation is used: each data set thus yields 10 models. The population variance and mean of the diagnostic statistics are calculated from the result of each set of 10 models applied to another data set. The resulting mean of the diagnostics will thus indicate the precision and correlation of the models used, while the variance indicate the robustness of using a model based on that set of data. The study methodology for this step is:

1. Divide data into sets of two (MCS and corresponding IMUS) and design linear and polynomial regression models using 10-fold cross-validation.
2. Apply all 10 polynomial and linear models designed after each set to all other sets.

Subjects	13
Male/female	5/8
Left/Right/double-handed	0/12/1
Age, mean\pm std [yrs]	62.25 \pm 13.36
Length, mean\pm std [m]	1.68 \pm 0.077
Arm length, mean\pm std [m]	0.5418 \pm 0.0467
Measurements	173

Table 3.4: The healthy participants of the study-population

3. Check the models robustness and precision by calculating population variance and mean of of the diagnostic statistics R^2 & RMSE.

3.8 Population and recruitment

The principles of recruitment are availability and convenience. Healthy subjects are pseudo-randomly picked from peers and social circles of the author (table 3.4). Individuals with stroke are picked from patients previously hospitalised at Sahlgrenska University hospital (table 3.5). The sample size consist of thirteen healthy individuals performing 10-15 measurements with each arm and three individuals with stroke performing 15 measurements with their affected arm. Approximately half of the trials have been deemed unfit for inclusion. The three major major reasons, of roughly equal significance and size, are as follows.

1. The IMUS failing to navigate properly.
2. Mismatched data-sets.
3. Failure of the MCS to spline the trajectory due to reflective markers being obscured.

The mismatched data sets occurred due to a weakness in the experimental procedure, which did not include a structured way of handling different amounts of data sets measured by the two systems from the same subject. When one system failed to produce data due to errors, different amounts of data sets would be available and thus yield errors. Since the data sets are to be compared between the systems, the potential mismatch warranted exclusion of affected data sets.

3.8.1 Inclusion and exclusion criteria for individuals with stroke

Inclusion criteria:

The individual is to have been clinically diagnosed with stroke, either infarction or

Subject	201 (S1)	202 (S2)	203 (S3)
Male/female	M	F	M
Age [yrs]	65	59	54
Length [m]	1.65	1.62	1.9
Arm length [m]	0.52	0.52	65
Left/Right-handed	R	R	R
Measurements unaffected/paretic arm	0/8	14/9	0/6
Time since stroke [yrs]	4	6	2
Paretic arm [Left/Right]	L	L	L
Ishemic/Hemorrhagic	H	I	I
FMA-UE 0-66, 66 indicates no clinical impairment	32	26	59
ARAT 0-57, 57 indicates no impairment/deficit	49	27	51

Table 3.5: The stroke participants of the study-population

bleeding, with resulting upper extremity sensorimotor impairment. The individual has to be able to understand and follow simple instructions. Upper extremity sensorimotor impairment is defined as scoring less than full score in a Modified Motor- or Fugl-Meyer -Assesment.

Exclusion criteria:

The individual must not be suffering from other neurological or musculoskeletal diseases/disorders that will affect the movement ability in the affected arm.

3.8.2 Inclusion and exclusion criteria for healthy individuals

Inclusion criteria:

The individual has to be above 39 years of age.

Exclusion criteria:

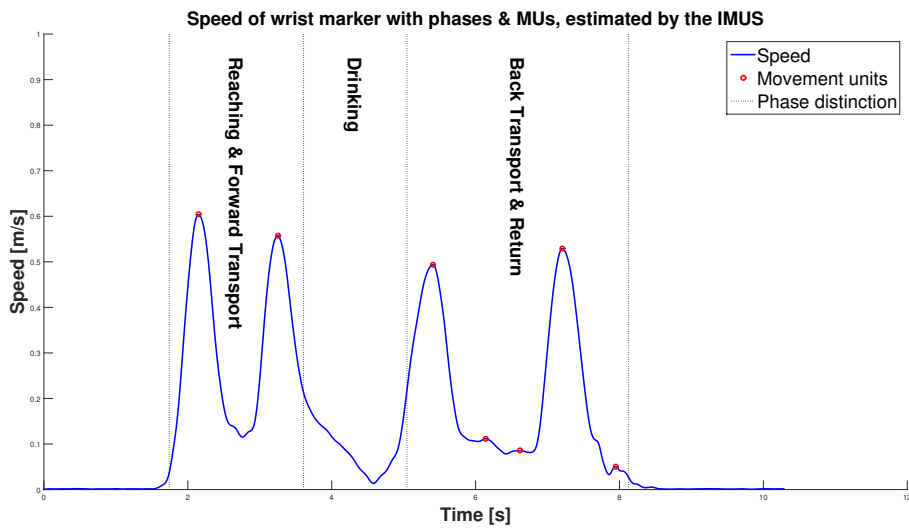
The individual must not be suffering from any disease or disorder which may hamper or affect the movement of the trunk or upper extremities.

4

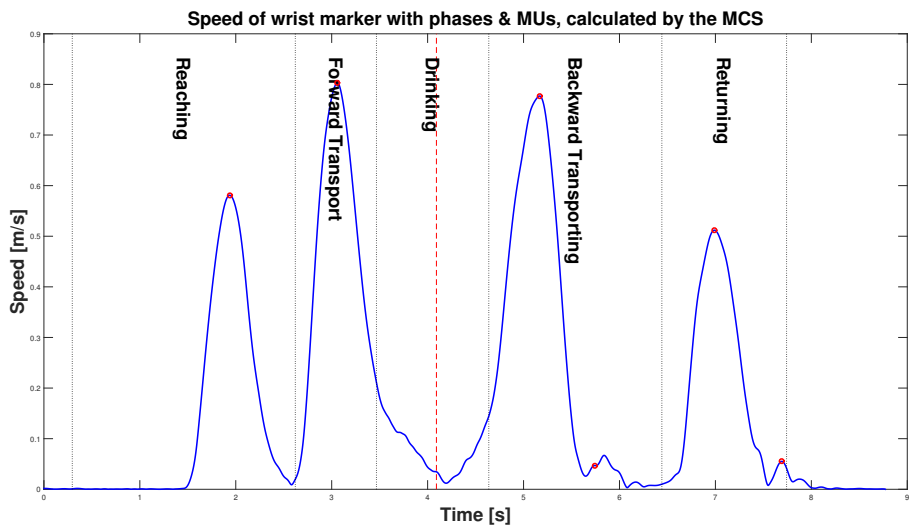
Results

4.1 Estimation quality and robustness

The IMUS's estimate of the speed vary in quality with respect to the MCS's estimates. The majority of the healthy samples result in IMUS and MCS estimates of comparable form and magnitude as can be observed in Figure: 4.1. The most prominent differences between such pairs are described in table: 4.1. Estimates of samples from stroke survivors are prone deviate more and usually lack a clear four-peak profile. A typical example of such a sample can be observed in figure: 4.3. The differences in estimates from affected samples are more difficult to quantify than those from healthy samples, though table: 4.1 is still relevant. Most notably the IMUS estimates from affected samples usually contain a higher number of small peaks with resulting MUs, which are not present in corresponding MCS estimate. Low quality estimates (figure: 4.2) are present both in healthy and affected samples. Signs of degeneration, such as arcs of a sector, speed over 1 m/s or other unrealistic behaviours (figure: 4.4), are also present in both affected and healthy samples. Low quality/degeneration in estimates are more common and prominent in samples from affected subjects.



(a) IMUS estimate.



(b) MCS estimate.

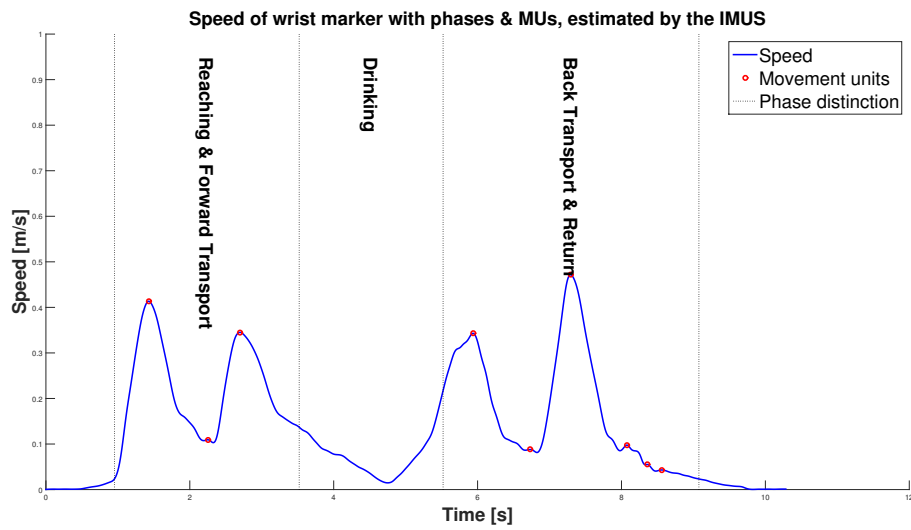
Figure 4.1: A pair of estimates from a healthy subject (H110), made by the MCS and IMUS, where the estimate of the IMUS contains small errors with respect to other estimates.

The different approaches of phase-estimation used in the two methods correspond in the case of healthy samples with a common level of estimation quality, save for the beginning of the reach phase. The phase-placements of most interest are: the beginning of the reach-phase (marking the beginning of the movement), the placement of the drinking-phase (in which MUs are not counted due to the high amount of MUs present) and the end of the return-phase (the end of the movement). Estimates from affected samples have larger differences in phase estimation. Erroneous estimates of the drinking-phase rarely give rise to large errors (different amount of MUs) in estimates with clear four-peak shape. This is due to the rarity of MUs in the end

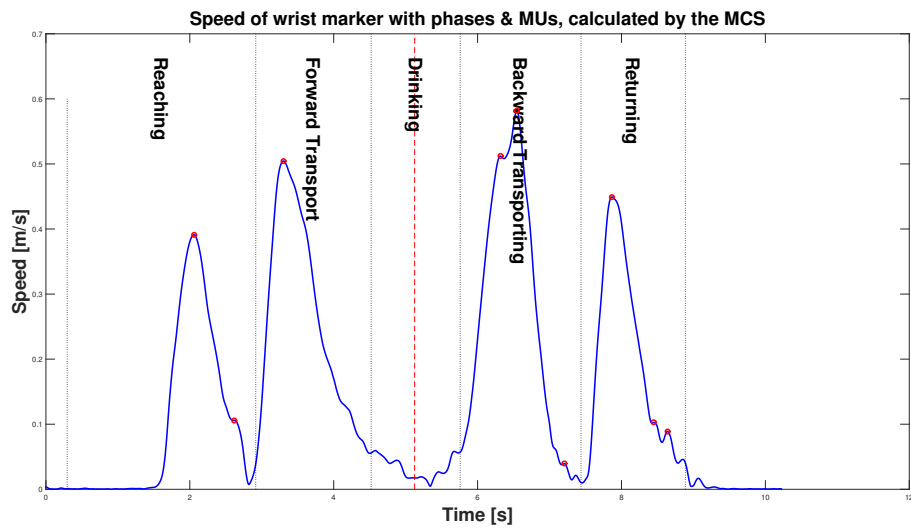
IMUS - deviation	MCS - normal case	Phase/location
Near equal top speed in all phases.	Higher speed in forward/backward transport phase.	Reach, return, forward and backward transport phases.
Non-zero speed outside drinking phase	Reaches zero between each phase.	Between the two transport phases and reach/return phases.
High number of low-amplitude peaks.	Smoother speed vector.	Most prominent by the end of the return-phase.
"V"-shaped speed in the drinking phase	Frequently reaches zero.	The drinking phase.
Split peaks/high frequency components.	Four peak profile.	Middle reach, return and forward/backward transport.

Table 4.1: Most common differences between the IMUS and MCS speed estimates.

of the forward transport-phase and the beginning of the backward transport-phase in such samples. In the case of a obscured four-peak shape due to poor estimation or high level of disability in the subject, the latter statement does not hold. Instead, the drinking-phase can be the source of large errors due to being placed in the wrong area. Identification of the beginning of the reach-phase differs between the algorithms, mostly due to the sensitivity of the tuning in the MCS (as can be observed in figure: 4.2). Different amounts of MUs due to the placement of the beginning of the reach-phase appears to have little effect. The time measurement is however affected. The end of the return phase is a source of errors, since the end of the movement commonly contains large numbers of peaks resulting in MUs. Though the MCS and IMUS differ little in this estimate, large errors can still be a by-product (as can be observed in Figure: 4.3).

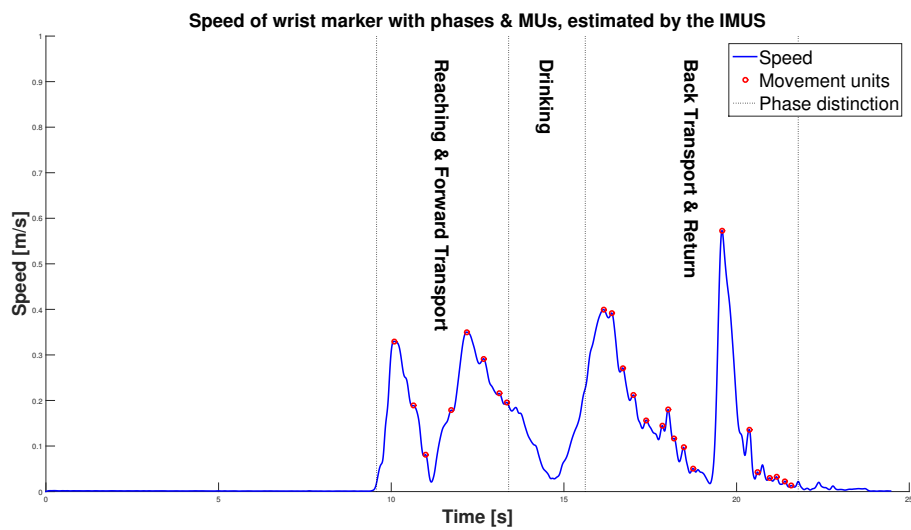


(a) IMUS estimate.

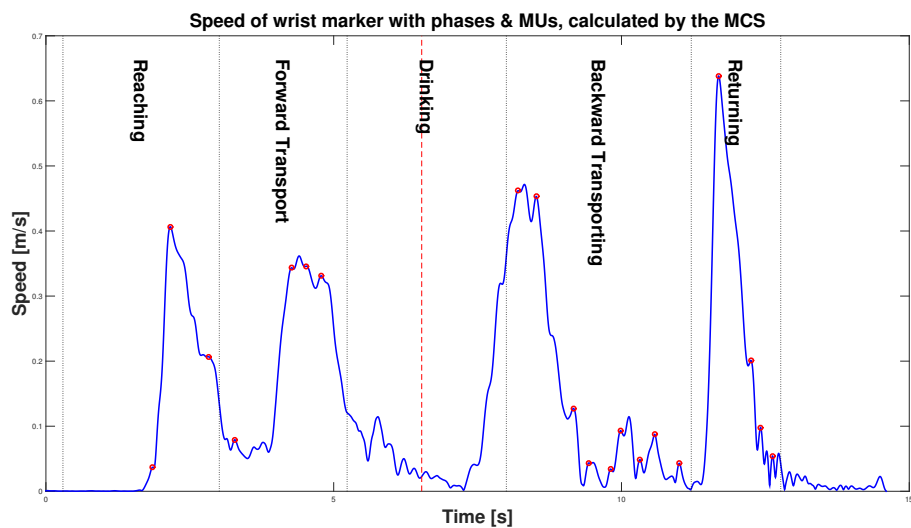


(b) MCS estimate.

Figure 4.2: A pair of estimates from a healthy subject (H110), made by the MCS and IMUS, where the estimate of the IMUS deviates and show noticeable errors. An example of a worse estimate with respect to other IMUS estimates.

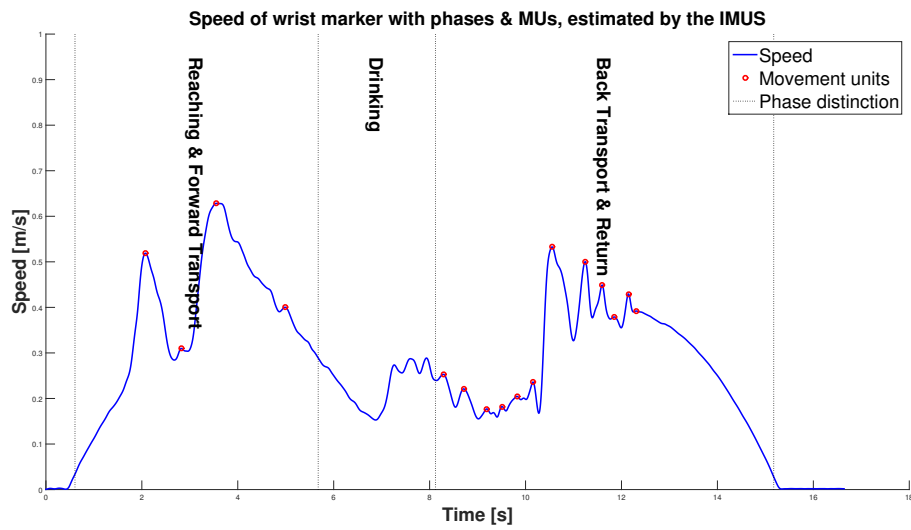


(a) IMUS estimate.

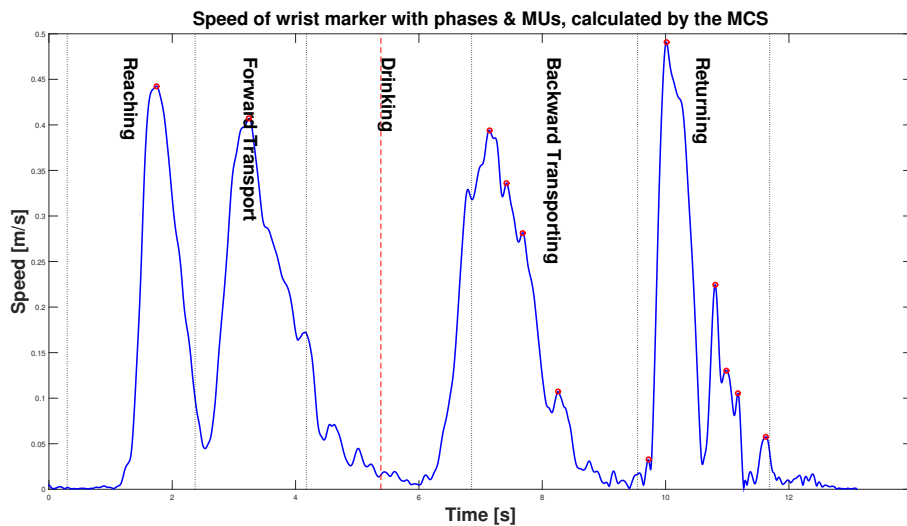


(b) MCS estimate.

Figure 4.3: A pair of estimates from a subject with stroke (S201), made by the MCS and IMUS, where the estimate of the IMUS contains small errors with respect to other estimates.

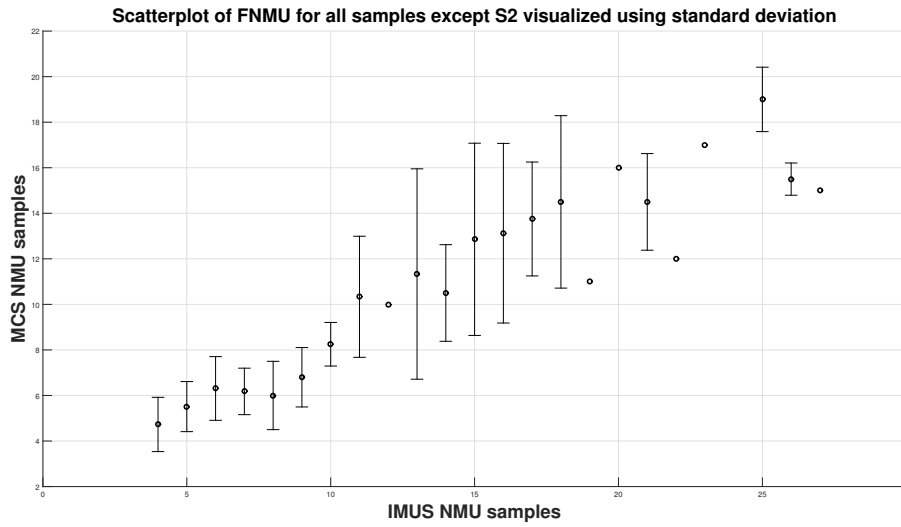


(a) IMUS estimate.

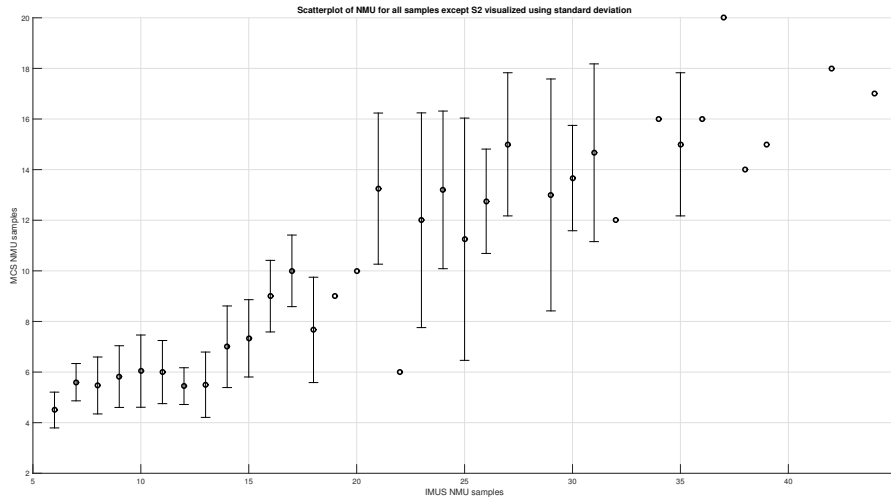


(b) MCS estimate.

Figure 4.4: A pair of estimates from a subject with stroke, made by the MCS and IMUS (S201), where the estimate of the IMUS deviates and show noticeable errors. An example of a worse estimate with respect to other IMUS estimates.



(a) IMUS:FNMU against MCS:NMU



(b) IMUS:NMU against MCS:NMU

Figure 4.5: Barplots featuring the standard-deviation of the MU features for all data.

4.2 Linear regression analysis

IMUS:NMU and FNMU show approximate linear correlation with MCS:NMU (see figures: 4.5, A.3 and A.5). Using 10-folds cross-validation, a linear model applied to IMUS:FNMU achieves better result with respect to other variables and models (see table: 4.2). All combinations of variables and models yield a R^2 of 0.8 or more and a mean RMSE of no more than 2.37 MU. IMUS:TMT correlates linearly with MCS:TMT (see appendix).

Samples from affected subjects appear to have other statistical moments than samples from healthy subjects. These non-linearities and variations between the sets are described in table: 4.3. This is directly observable in appendix figures: A.2 & A.1. The IMUS two MU-measures are characterised by having higher mean and std than MCS:NMU. IMUS:FNMU has a smaller std than IMUS:NMU (3.88 and 4.46 against 6.53 and 7.31 for affected and healthy samples respectively) and lower population mean, more akin to that of MCS:NMU. Inclusion of S2 in the set leads to increased mean and std (see table: A.2 and A.1). The effects of the variations are quantified and described by varying model fit in tables: A.7, A.4 & A.5 using the notation described in table: A.3, where models are applied to data not used to design them. The latter identifies large difference between S2 and all other groups. Its inclusion or exclusion has larger effect on model fit than the choice between samples from affected or non-affected arms, in most cases resulting in worse model fit. Model fit is more variable for polynomial models and is on average better for IMUS:FNMU than IMUS:NMU. It varies strongly for models trained on only affected data and applied to samples from healthy subjects or the other way around.

Variable/Measure	Mean RMSE	Mean R^2
Linear FNMU	2.15	0.83
Polynomial FNMU	2.24	0.83
Linear NMU	2.37	0.80
Polynomial NMU	2.30	0.82

Table 4.2: Mean RMSE and R^2 for polynomial and linear regression models created using 10-fold cross-validation on all a affected (14) samples and a equal number of random healthy samples (14). Total 28 samples.

Samples/ Variables	IMUS			MCS	
	TMT	NMU	FNMU	TMT	NMU
Healthy	8.01 ± 1.71	13.32 ± 7.31	8.00 ± 4.46	6.94 ± 1.53	7.21 ± 3.18
Affected	12.78 ± 1.54	30.79 ± 6.53	19.00 ± 3.88	11.10 ± 1.26	14.79 ± 3.17

Table 4.3: Mean and population standard deviation for the kinematic variables sorted by level of motor-impairment.

5

Discussion

The findings show that both IMUS:TMT, NMU and FNMU correlates well with the corresponding MCS variables, which is largely expected. The reconstructions and phase estimations made by the IMUS clearly relates to those of the MCS. The MU features of the IMUS show clear correlation with the MCS:NMU. However, the IMUS estimation quality is clearly unsteady, varying between high degree of likeness to only inheriting basic features. The inherent sensitivity of the MU definition creates a scenario where very small errors can give rise to additional MUs. The IMUS thus estimates a varying (compared to the MCS) amount of MUs even when the speed estimate is close to a correct representation of the physical reality. There are cases where the MCS and IMUS estimates the same amount of MUs, but at different locations, clearly showcasing a flaw in the approach. The IMUS would need an almost perfect estimate of the speed to find the same amount of MUs at the same location.

A mean RMSE of 2.15 and R^2 of 0.83 is achievable when using FNMU as predictor in a linear regression model and applying it to a equal measure of samples from affected and healthy subjects. The mean and standard deviation of MCS:NMU is 14.8 ± 3.17 (table: 4.3) for affected subjects. The corresponding values in earlier works are 11.1 ± 3.6 (FMA-UE 39-57) [20]. A RMSE of 2.15 when predicting MCS:NMU is thus a significant error, but would likely be small enough to clearly discern between affected and non-affected subjects. Significantly better or worse results can be achieved by creating models from subsets of the data, and applying them to other sets, revealing differences and non-linearities. Primarily between samples drawn from healthy subjects, affected subjects and S2. A RMSE of (table A.7) 1.89 and R^2 of 0.72 is reachable using a 2^{nd} degree polynomial model trained and applied to all FNMU data, with the exception of S2. The same models applied to the affected arms of the affected subjects result in RMSE 2.34 and R^2 0.45. Models trained on the affected arms result in a meagre improvement of precision for predicting the training data and severe deterioration for other data. The proposed models can thus not explain all variations in the data, and is better at predicting data from healthy rather than affected subjects, due to the smaller spread of the former. The same conclusion can be drawn from observing the scatterplots (figures: A.2 & A.1) or simply comparing the standard deviations of sets constructed from affected/healthy samples respectively (table: 4.3). The data derived from S2 can thus be concluded to differ from all other data, clearly having a different mean and appearing to have larger variance than other sets. No other previous works have evaluated subjects with as severely impaired motor function as S2 for the given task, setting the resulting data set apart from the other sets, all whom are within the boundaries of previous works. Furthermore, S2 was collected using a modified procedure. It's thus not implausible to consider S2 apart from the other data. Solely considering S2's level of motor impairment, the overall bad model fit warrants more intricate models than those proposed. The ramifications would thus be that the proposed models are only valid for subjects with motor-impairment ranging from moderate to none. The fact that the changed procedure rather than the higher level of impairment may be the source of the variation of the data is a moot point from a practical modelling perspective. A motor-impairment level greater than moderate implies the inability to complete the original procedure, rendering the models impractical for

any subject with impairment greater than moderate regardless of underlying cause.

The TMT features unsurprisingly show high levels of correlation, R^2 of 0.97 and RMSE of 0.45 (table A.6) when trained by and applied to all data. There is a deterioration of model fit when applied to data from affected subjects, primarily of RMSE (0.69), but the overall fit still appears to be good since 92% of the variations can be explained by the model. This pattern is repeated for all results: sets characterised by small sample size and inclusion of S2 result in worse fit with roughly 0.7 RMSE and 0.9 R^2 while other sets have RMSE around 0.45 and slightly higher R^2 .

The results give reasons to believe the system could be of use, but would need further evaluation. Using the same methods as the MCS would be the first step, meaning multivariate linear regression with the variables MCS:NMU, TMT & trunk displacement models. The first obstacle in this would be to find a substitute variable for trunk displacement, which could then be used in tandem to design and evaluate a multivariate model similar to that applied to the MCS. While the total trunk displacement would be likely to be less sensitive than the MU measure, problems with degenerated speed estimates and sensitivities of MUs could prove insurmountable problems. Should the precision of the IMUS be too low to achieve a useful predictive power, the estimates of the trajectories would need to be improved. The sensor errors could be improved using sensors of higher precision or evaluating the method of calibration and possibly improve it. The system also suffers from an initial position-problem due to a lack of information. To solve it, either the procedure would need to include a specific start position and location of the IMU, or the IMUS would need to be fitted with an absolute orientation algorithm. Such an algorithm would require the IMU to be fitted with a magnetometer or similar sensor, since a (low precision) gyroscope and accelerometer doesn't supply enough information to find the absolute orientation of a system. Other approaches to improve the estimate of the trajectory would be possible. A sensor capable of tracking an external reference could potentially help attenuate and even reduce the ever-growing errors of the inertial navigation. It's also possible that it would be more efficient to derive information directly from the accelerometer/gyroscope data rather than the trajectory estimate. Such an approach would require identifying new sets of features, but would not suffer from the inherent problems of the dead reckoning systems such as increasing errors over time.

6

Conclusion

The IMUS:FNMU/NMU features of the IMUS correlates with those of the MCS and can be used to predict the latter with an error (RMSE of 2.15 for FNMU) likely to be smaller than the difference between sick and healthy individuals. The IMUS estimates have varying quality. They commonly result in a matching profile when compared with the MCS, but show signs of degeneration and deviation at a notable number of times. These deviations are especially prominent in estimates from samples of affected subjects. The estimates are unlikely to have matching temporal locations for MUs, even when the estimates have highly comparable profile. This disparity indicates that predictions with high (next-to-perfect) precision would demand a considerably enhanced IMUS estimate. The estimates of the total time show high levels of correlation and precision. No final conclusion can be drawn whether the precision is good enough without emulating the whole MCS method in the IMUS. That would require implementing the features in a multivariate linear regression model trained to predict ARAT-scores (and a significantly larger sample size). Such an approach would require the identification of a trunk displacement feature replacement for the IMUS. Finding the latter is the primary challenge remaining before the system can be fully compared and evaluated against the MCS.

Bibliography

- [1] Corbyn Z. A growing global burden. *Nature*. 2014;510(7506):S2
- [2] Johnston S. Global variation in stroke burden and mortality: estimates from monitoring, surveillance, and modelling. *Lancet Neurol*. 2009;8(4):345-54.
- [3] Alt Murphy, Margit. Development and validation of upper extremity kinematic movement analysis for people with stroke. Reaching and drinking from a glass. GUPEA [internet]. 2013 Nov [cited 2016 May] PhD thesis. Available from: <https://gupea.ub.gu.se/handle/2077/33117?locale=sv>
- [4] Nichols-Larsen DS, Clark PC, Zeringue A, Greenspan A, Blanton S. Factors influencing stroke survivors' quality of life during subacute recovery. *Stroke; a journal of cerebral circulation*. 2005;36(7):1480-4.
- [5] Stucki G, Reinhardt JD, Grimby G, Melvin J. Developing "Human Functioning and Rehabilitation Research" from the comprehensive perspective. *J Rehabil Med*. 2007;39:665-671.
- [6] Fugl-Meyer AR, Jaasko L, Leyman I, Olsson S, Steglind S. The post-stroke hemiplegic patient. 1. a method for evaluation of physical performance. *Scand J Rehabil Med* 1975; 7(1): 13-31.
- [7] Lyle RC. A performance test for assessment of upper limb function in physical rehabilitation treatment and research. *International Journal of Rehabilitation Research*. 1981;4(4):483-92.
- [8] Chèze L, Ebrary (e-book collection). *Kinematic analysis of human movement*. 1st ed. London: ISTE; 2014
- [9] Norris M, Anderson R, Kenny IC. Method analysis of accelerometers and gyroscopes in running gait: A systematic review. Proceedings of the Institution of Mechanical Engineers, *Part P: Journal of Sports Engineering and Technology*. 2014;228(1):3-15.
- [10] Tao X, SpringerLink (Online service), SpringerLink (e-book collection). *Handbook of Smart Textiles*. 1st 2015; ed. Singapore: Springer Singapore.
- [11] Mayagoitia RE, Nene AV, Veltink PH. Accelerometer and rate gyroscope measurement of kinematics: an inexpensive alternative to optical motion analysis systems. *Journal of Biomechanics*. 2002;35(4):537-42.

- [12] Perdikaris GA, SpringerLink (Online service), SpringerLink Archive (e-book collection). *Computer Controlled Systems: Theory and Applications*. Dordrecht: Springer Netherlands; 1991.
- [13] Murphy, Margit Alt, Carin Willén, and Katharina S. Sunnerhagen. "Movement kinematics during a drinking task are associated with the activity capacity level after stroke." *Neurorehabilitation and neural repair* 26.9 (2012): 1106-1115.
- [14] Julier, Simon J., and Jeffrey K. Uhlmann. "New extension of the Kalman filter to nonlinear systems." *AeroSense'97*. International Society for Optics and Photonics, 1997.
- [15] Kovvali N, Banavar M, Spanias A, Morgan & Claypool. *Introduction to Kalman Filtering with MATLAB examples*. 1st ed. San Rafael, California: Morgan Claypool Publishers; 2014;
- [16] Zarchan P, Musoff H, Ebrary (e-book collection). *Fundamentals of Kalman filtering: a practical approach*. 2nd ed. Reston, Va: American Institute of Aeronautics and Astronautics; 2005
- [17] Van Der Merwe, Ronell, and Eric A. Wan. "The square-root unscented Kalman filter for state and parameter-estimation." *Acoustics, Speech, and Signal Processing, 2001. Proceedings.(ICASSP'01)*. 2001 IEEE International Conference on. Vol. 6. IEEE, 2001.
- [18] Rauch He, Striebel Ct, Tung F. Maximum likelihood estimates of linear dynamic systems. *AIAA Journal*. 1965;3(8):1445-50.
- [19] Titterton DH, Weston JL. *Strapdown inertial navigation technology*. 2.;2nd; ed. Stevenage: IEE; 2006;.
- [20] Murphy MA, Willén C, Sunnerhagen KS, et al. Kinematic Variables Quantifying Upper-Extremity Performance After Stroke During Reaching and Drinking From a Glass. *Neurorehabilitation and Neural Repair*. 2011;25(1):71-80.
- [21] Persson HC, Alt Murphy M, Danielsson A, Lundgren-Nilsson Å, Sunnerhagen KS, et al. A cohort study investigating a simple, early assessment to predict upper extremity function after stroke - a part of the SALGOT study. *BMC neurology*. 2015;15:92.
- [22] Simo Särkkä. Bayesian filtering and smoothing. Cambridge: *Cambridge University Press*; 2013.

A

Appendix 1

A.1 Moments of MU-sets

Set/Var	MCS:NMU	IMUS:NMU	IMUS:FNMU
Set 1	7.2±3.2	13.3±7.3	8.0±4.5
Set 2	28.1±17.5	39.3±12.7	27.6±11.6
Set 3	16.4±2.3	31.1±6.6	20.4±4.4
Set 4	47.3±9.0	51.6±8.2	39.9±6.2
Set 5	12.7±3.0	30.3±7.1	17.2±2.3
Set 7	5.8±1.5	10.7±2.3	5.9±0.9
Set 14	5.5±0.9	8.6±1.8	5.4±0.7
Set 15	5.5±1.1	10.4±1.8	6.3±1.2
Set 18	14.1±2.8	28.1±6.4	17.3±4.2
Set 20	14.8±3.3	30.8±6.5	19±3.9
Set 21	11.1±4.8	21.3±10.8	13.2±6.7

Table A.1: Moments of the sets for the MU-variables, on the form mean±std.

Group	Subjects
Set 1	Healthy
Set 2	Stroke
Set 3	S1
Set 4	S2
Set 5	S3
Set 7	H2
Set 14	H9
Set 15	H11
Set 18	H11
Set 20	S1 & S3
Set 21	H9 & H14

Table A.2: Notation of set-divisions used to detail the moments of the MU-distributions

Group	Subjects
Group 1	All data
Group 2	Stroke (S2 included)
Group 3	Affected, both arms
Group 4	Healthy
Group 5	All data (S2 excluded)
Group 6	Stroke (S2 excluded)

Table A.3: Notation of set-divisions used to train and test regression models

A.2 Polynomial and linear regression-models

Training group 1	group 1	group 2	group 3	group 4	group 5	group 6
Mean RMSE	4.66	11.35	9.10	2.99	3.29	6.01
Variance RMSE	0.0000	0.0888	0.0476	0.0170	0.0229	0.1411
Mean R^2	0.73	0.56	0.72	0.11	0.17	-2.61
Variance R^2	0.0000	0.0005	0.0002	0.0059	0.0057	0.1979
Training group 2	group 1	group 2	group 3	group 4	group 5	group 6
Mean RMSE	13.32	9.79	10.31	13.86	13.40	8.46
Variance RMSE	1.7864	0.0876	0.4747	2.0874	1.8979	0.1867
Mean R^2	-1.22	0.67	0.64	-18.28	-12.83	-6.17
Variance R^2	0.2236	0.0004	0.0025	18.2840	9.1454	0.5423
Training group 3	group 1	group 2	group 3	group 4	group 5	group 6
Mean RMSE	6.36	9.67	7.99	5.95	5.98	7.71
Variance RMSE	0.2063	0.0239	0.0063	0.3452	0.3096	0.3003
Mean R^2	0.50	0.68	0.78	-2.55	-1.75	-4.96
Variance R^2	0.0054	0.0001	0.0000	0.5088	0.2692	0.6731
Training group 4	group 1	group 2	group 3	group 4	group 5	group 6
Mean RMSE	6.04	17.82	14.01	1.79	1.94	3.02
Variance RMSE	0.0042	0.0441	0.0259	0.0000	0.0000	0.0045
Mean R^2	0.55	-0.09	0.33	0.68	0.71	0.09
Variance R^2	0.0001	0.0007	0.0002	0.0000	0.0000	0.0017
Training group 5	group 1	group 2	group 3	group 4	group 5	group 6
Mean RMSE	5.95	17.55	13.80	1.79	1.94	2.97
Variance RMSE	0.0047	0.0527	0.0305	0.0000	0.0000	0.0032
Mean R^2	0.56	-0.05	0.35	0.68	0.71	0.12
Variance R^2	0.0001	0.0008	0.0003	0.0000	0.0000	0.0011
Training group 6	group 1	group 2	group 3	group 4	group 5	group 6
Mean RMSE	6.31	17.35	13.78	2.85	2.94	2.74
Variance RMSE	0.3860	0.7503	0.5754	0.8041	0.7083	0.0081
Mean R^2	0.50	-0.03	0.35	0.12	0.29	0.25
Variance R^2	0.0099	0.0105	0.0050	0.3220	0.1741	0.0025

Table A.4: Performance of linear regression for NMU with NMU as predictor

Training group 1	group 1	group 2	group 3	group 4	group 5	group 6
Mean RMSE	3.67	8.30	6.55	2.71	2.80	4.53
Variance RMSE	0.0000	0.0299	0.0175	0.0039	0.0058	0.0520
Mean R^2	0.83	0.76	0.85	0.27	0.40	-1.05
Variance R^2	0.0000	0.0001	0.0000	0.0011	0.0011	0.0414
Training group 2	group 1	group 2	group 3	group 4	group 5	group 6
Mean RMSE	3.78	8.82	6.96	2.68	2.69	3.60
Variance RMSE	0.0004	0.0653	0.0360	0.0165	0.0161	0.0216
Mean R^2	0.82	0.73	0.84	0.28	0.45	-0.30
Variance R^2	0.0000	0.0002	0.0001	0.0051	0.0029	0.0121
Training group 3	group 1	group 2	group 3	group 4	group 5	group 6
Mean RMSE	4.15	7.46	5.98	3.66	3.72	5.45
Variance RMSE	0.0221	0.0018	0.0003	0.0405	0.0363	0.0599
Mean R^2	0.79	0.81	0.88	-0.34	-0.06	-1.97
Variance R^2	0.0002	0.0000	0.0000	0.0222	0.0120	0.0691
Training group 4	group 1	group 2	group 3	group 4	group 5	group 6
Mean RMSE	5.21	15.09	11.83	1.91	1.92	2.49
Variance RMSE	0.0134	0.1433	0.0866	0.0000	0.0001	0.0178
Mean R^2	0.66	0.22	0.52	0.64	0.72	0.38
Variance R^2	0.0002	0.0016	0.0006	0.0000	0.0000	0.0046
Training group 5	group 1	group 2	group 3	group 4	group 5	group 6
Mean RMSE	4.99	14.38	11.28	1.91	1.91	2.31
Variance RMSE	0.0097	0.1098	0.0663	0.0000	0.0000	0.0071
Mean R^2	0.69	0.29	0.57	0.64	0.72	0.47
Variance R^2	0.0002	0.0011	0.0004	0.0000	0.0000	0.0015
Training group 6	group 1	group 2	group 3	group 4	group 5	group 6
Mean RMSE	4.99	13.82	10.88	2.29	2.27	2.21
Variance RMSE	0.1615	1.6475	1.0461	0.1446	0.1355	0.0055
Mean R^2	0.69	0.34	0.59	0.46	0.60	0.51
Variance R^2	0.0025	0.0132	0.0052	0.0326	0.0177	0.0011

Table A.5: Performance of linear regression for NMU with FNMU as predictor

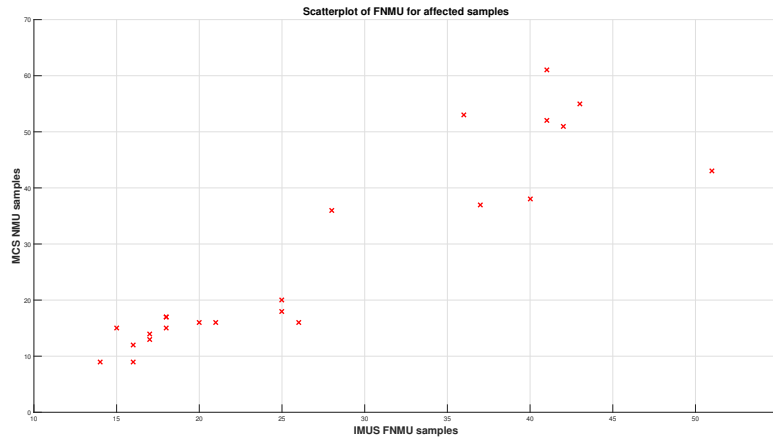
Training group 1	group 1	group 2	group 3	group 4	group 5	group 6
Mean RMSE	0.45	0.69	0.62	0.41	0.41	0.40
Variance RMSE	0.00000	0.00006	0.00003	0.00000	0.00000	0.00011
Mean R^2	0.97	0.92	0.97	0.93	0.95	0.90
Variance R^2	0.00000	0.00000	0.00000	0.00000	0.00000	0.00003
Training group 2	group 1	group 2	group 3	group 4	group 5	group 6
Mean RMSE	0.58	0.67	0.66	0.56	0.56	0.45
Variance RMSE	0.00507	0.00006	0.00105	0.00649	0.00585	0.00057
Mean R^2	0.94	0.93	0.96	0.86	0.90	0.87
Variance R^2	0.00023	0.00000	0.00001	0.00171	0.00083	0.00020
Training group 3	group 1	group 2	group 3	group 4	group 5	group 6
Mean RMSE	0.46	0.68	0.61	0.43	0.44	0.52
Variance RMSE	0.00008	0.00013	0.00005	0.00010	0.00010	0.00123
Mean R^2	0.96	0.93	0.97	0.92	0.94	0.83
Variance R^2	0.00000	0.00001	0.00000	0.00001	0.00001	0.00055
Training group 4	group 1	group 2	group 3	group 4	group 5	group 6
Mean RMSE	0.47	0.83	0.72	0.40	0.40	0.36
Variance RMSE	0.00002	0.00050	0.00026	0.00000	0.00000	0.00002
Mean R^2	0.96	0.89	0.96	0.93	0.95	0.92
Variance R^2	0.00000	0.00004	0.00000	0.00000	0.00000	0.00001
Training group 5	group 1	group 2	group 3	group 4	group 5	group 6
Mean RMSE	0.47	0.80	0.70	0.40	0.40	0.35
Variance RMSE	0.00001	0.00047	0.00024	0.00000	0.00000	0.00001
Mean R^2	0.96	0.90	0.96	0.93	0.95	0.92
Variance R^2	0.00000	0.00003	0.00000	0.00000	0.00000	0.00000

Table A.6: Performance of linear regression with for TMT

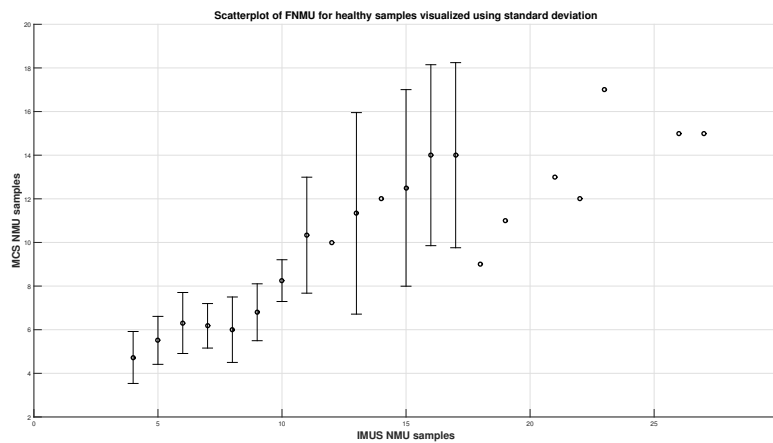
Training group 1	group 1	group 2	group 3	group 4	group 5	group 6
Mean RMSE	3.26	7.95	6.27	2.16	2.16	2.86
Variance RMSE	0.0099	0.1465	0.0873	0.0013	0.0018	0.0183
Mean R^2	0.87	0.78	0.87	0.54	0.64	0.18
Variance R^2	0.0001	0.0005	0.0002	0.0002	0.0002	0.0057
Training group 2	group 1	group 2	group 3	group 4	group 5	group 6
Mean RMSE	14.48	6.98	10.66	15.12	14.62	5.07
Variance RMSE	14.8981	0.2429	2.7569	18.5519	17.2128	0.3378
Mean R^2	-1.77	0.83	0.61	-23.38	-16.51	-1.59
Variance R^2	1.1770	0.0007	0.0120	96.8866	49.8822	0.3016
Training group 3	group 1	group 2	group 3	group 4	group 5	group 6
Mean RMSE	3.91	7.66	6.11	3.25	3.27	4.50
Variance RMSE	0.0373	0.3101	0.1621	0.1729	0.1693	0.2420
Mean R^2	0.81	0.80	0.87	-0.07	0.17	-1.04
Variance R^2	0.0004	0.0010	0.0003	0.0654	0.0382	0.1750
Training group 4	group 1	group 2	group 3	group 4	group 5	group 6
Mean RMSE	7.17	21.45	16.79	1.87	1.92	2.81
Variance RMSE	0.0862	0.8718	0.5320	0.0000	0.0002	0.0237
Mean R^2	0.36	-0.58	0.04	0.65	0.72	0.21
Variance R^2	0.0027	0.0186	0.0068	0.0000	0.0000	0.0073
Training group 5	group 1	group 2	group 3	group 4	group 5	group 6
Mean RMSE	6.14	18.14	14.21	1.88	1.89	2.34
Variance RMSE	0.0228	0.2401	0.1461	0.0000	0.0000	0.0044
Mean R^2	0.53	-0.13	0.31	0.65	0.73	0.45
Variance R^2	0.0005	0.0037	0.0014	0.0000	0.0000	0.0010
Training group 6	group 1	group 2	group 3	group 4	group 5	group 6
Mean RMSE	12.61	28.88	23.15	8.65	8.32	2.03
Variance RMSE	41.8716	80.7404	60.5905	44.3696	41.0795	0.0176
Mean R^2	-1.44	-2.10	-1.01	-10.41	-7.10	0.59
Variance R^2	8.6873	4.3148	2.1992	387.5779	196.5920	0.0030

Table A.7: Performance of polynomial regression models using FNMU as training data to predict NMU

A.3 Scatterplots

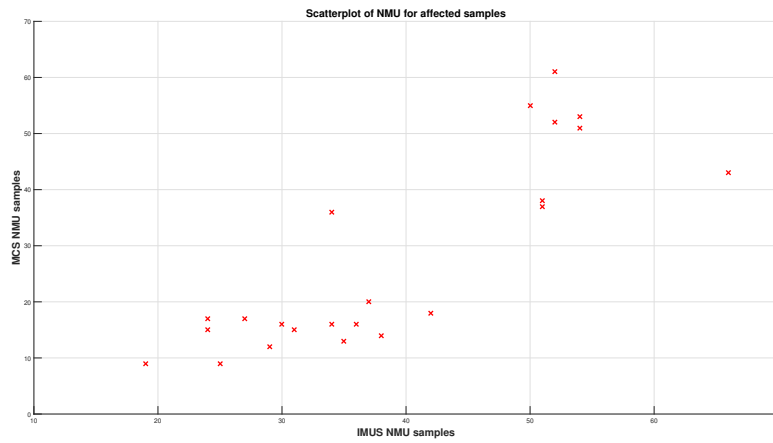


(a) Scatterplot of affected IMUS:FNMU against MCS:NMU

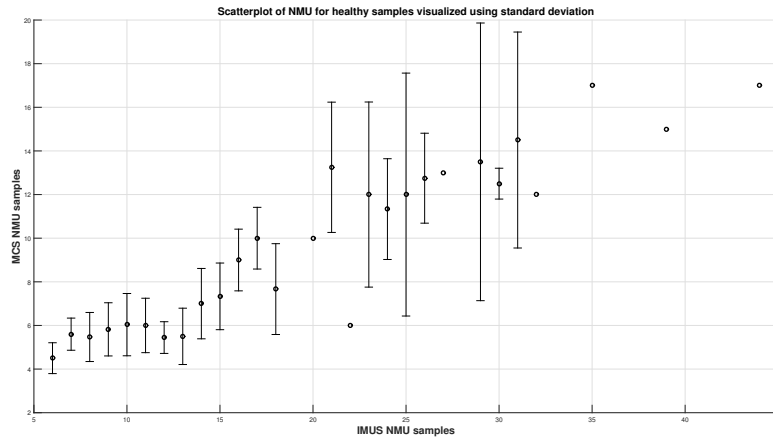


(b) Barplot of healthy IMUS:FNMU against MCS:NMU

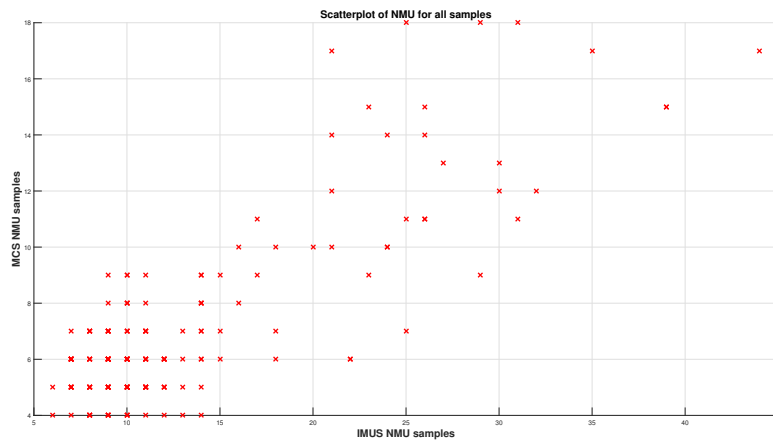
Figure A.1: FNMU scatter/bar-plots of the affected and healthy samples respectively.



(a) Scatterplot of affected IMUS:NMU against MCS:NMU

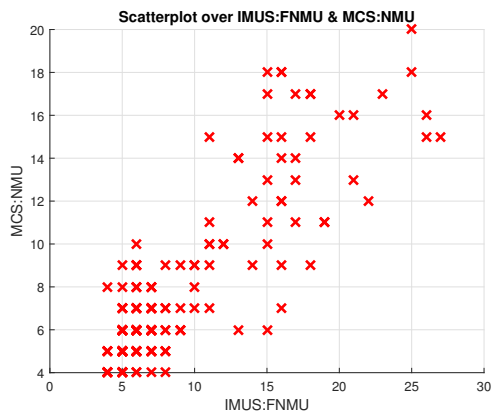


(b) Barplot of healthy IMUS:NMU against MCS:NMU

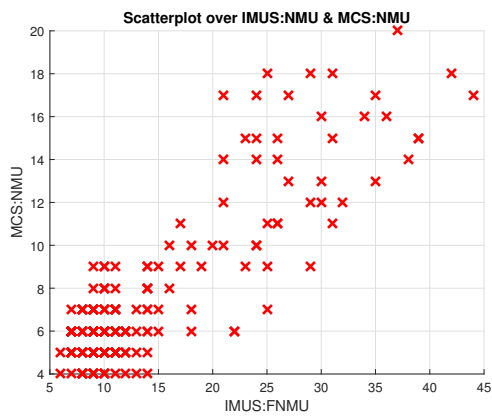


(c) Scatterplot of healthy IMUS:NMU against MCS:NMU

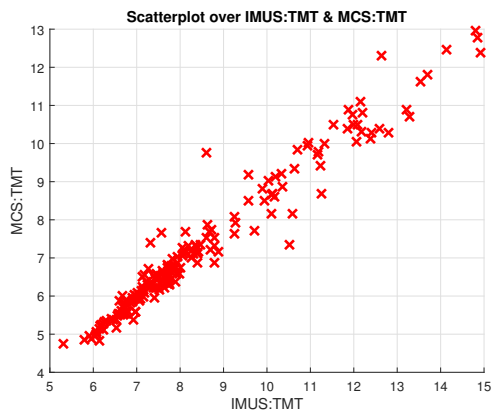
Figure A.2: NMU scatter/bar-plots of the affected and healthy samples respectively.



(a) Scatterplot of IMUS:FNMU against MCS:NMU



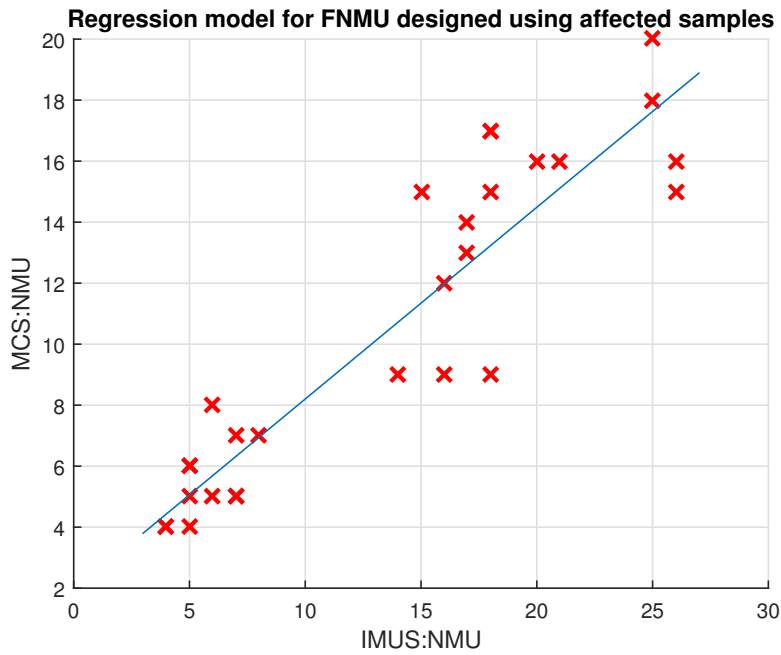
(b) Scatterplot of IMUS:NMU against MCS:NMU



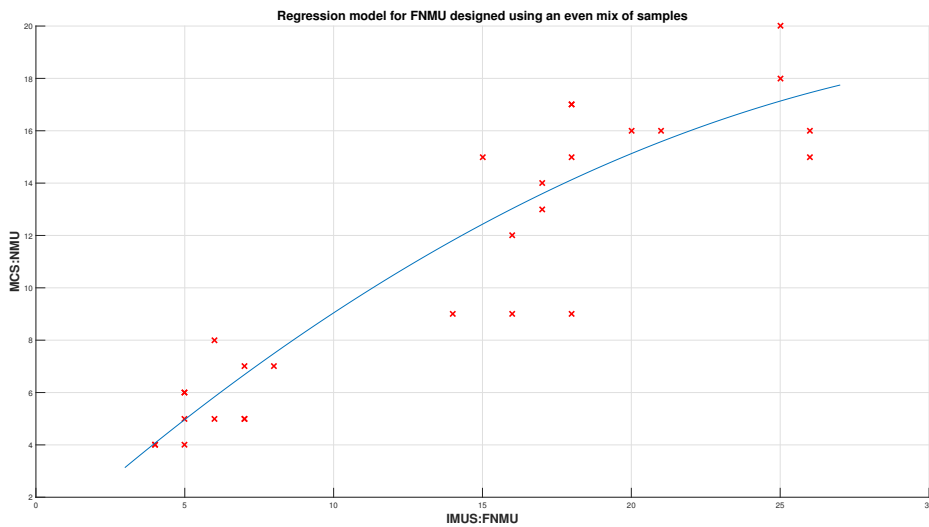
(c) Scatterplot of IMUS:TMT against MCS:TMT

Figure A.3: Scatterplots of the three different features.

A.4 Linear regression graphs

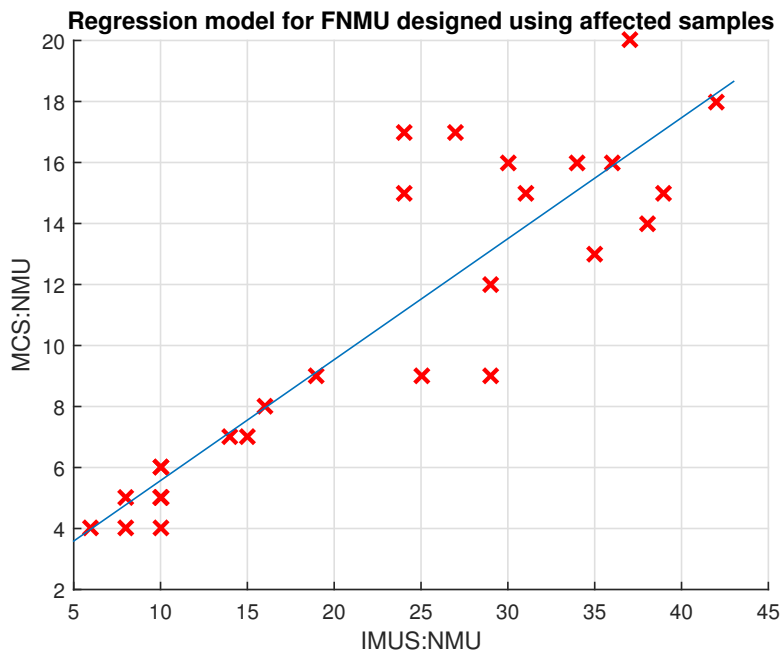


(a) Linear regression for a linear model fitted against IMUS:FNMU/MCS:NMU-data. The samples consist of 14 affected samples (S2 excluded) and 14 randomly picked healthy samples.

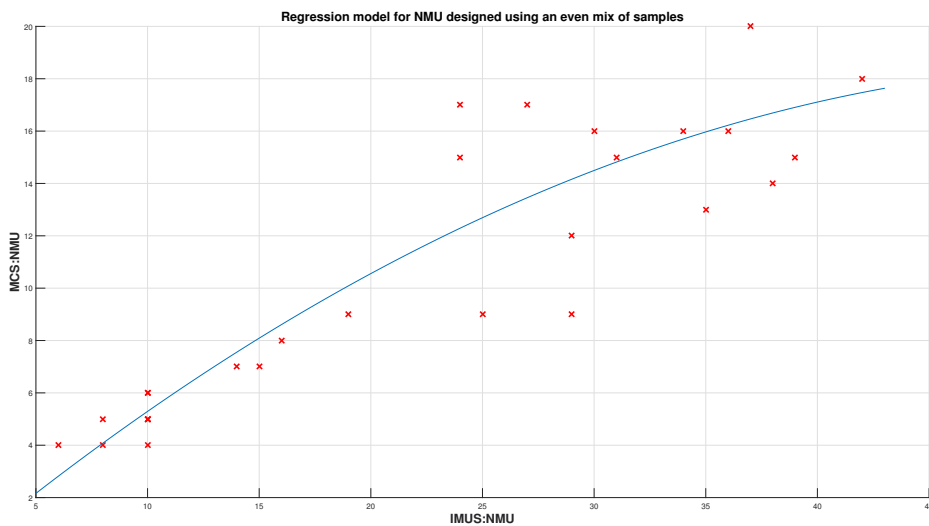


(b) Linear regression for a 2nd order polynomial model fitted against IMUS:FNMU/MCS:NMU-data. The samples consist of 14 affected samples (S2 excluded) and 14 randomly picked healthy samples.

Figure A.4: Regression models predicting MCS:NMU using IMUS:FNMU.



(a) Linear regression for a linear model fitted against IMUS:NMU/MCS:NMU-data. The samples consist of 14 affected samples (S2 excluded) and 14 randomly picked healthy samples.



(b) Linear regression for a 2nd order polynomial model fitted against IMUS:NMU/MCS:NMU-data. The samples consist of 14 affected samples (S2 excluded) and 14 randomly picked healthy samples.

Figure A.5: Regression models predicting MCS:NMU using IMUS:NMU.